DOI:10.1093/jnci/djt006
Advance Access publication February 27, 2013

ARTICLE

Targeting Primitive Chronic Myeloid Leukemia Cells by Effective Inhibition of a New AHI-1–BCR-ABL–JAK2 Complex

Min Chen, Paolo Gallipoli, Donna DeGeer, Ivan Sloma, Donna L. Forrest, Matthew Chan, Damian Lai, Heather Jorgensen, Ashley Ringrose, Hui Mi Wang, Karen Lambie, Helen Nakamoto, Kyi Min Saw, Ali Turhan, Ralph Arlinghaus, James Paul, Jon Stobo, Michael J. Barnett, Allen Eaves, Connie J Eaves, Tessa L. Holyoake, Xiaoyan Jiang

Manuscript received April 23, 2012; revised July 25, 2012; accepted January 3, 2013.

Correspondence to: Xiaoyan Jiang, MD, PhD, Terry Fox Laboratory, BC Cancer Agency, 675 W 10th Ave, Vancouver, BC, V5Z 1L3, Canada (e-mail: xjiang@bccrc.ca).

Background Imatinib mesylate (IM) induces clinical remission of chronic myeloid leukemia (CML). The Abelson helper integration site 1 (AHI-1) oncoprotein interacts with BCR-ABL and Janus kinase 2 (JAK2) to mediate IM response of primitive CML cells, but the effect of the interaction complex on the response to ABL and JAK2 inhibitors is unknown.

Methods The AHI-1–BCR-ABL–JAK2 interaction complex was analyzed by mutational analysis and coimmunoprecipitation. Roles of the complex in regulation of response or resistance to ABL and JAK2 inhibitors were investigated in *BCR-ABL*$^+$ cells and primary CML stem/progenitor cells and in immunodeficient NSG mice. All statistical tests were two-sided.

Results The WD40-repeat domain of AHI-1 interacts with BCR-ABL, whereas the N-terminal region interacts with JAK2; loss of these interactions statistically significantly increased the IM sensitivity of CML cells. Disrupting this complex with a combination of IM and an orally bioavailable selective JAK2 inhibitor (TG101209 [TG]) statistically significantly induced death of *AHI-1*–overexpressing and IM-resistant cells in vitro and enhanced survival of leukemic mice, compared with single agents (combination vs TG alone: 63 vs 53 days, ratio = 0.84, 95% confidence interval [CI] = 0.6 to 1.1, $P = .004$; vs IM: 57 days, ratio = 0.9, 95% CI = 0.61 to 1.2, $P = .003$). Combination treatment also statistically significantly enhanced apoptosis of CD34$^+$ leukemic stem/progenitor cells and eliminated their long-term leukemia-initiating activity in NSG mice. Importantly, this approach was effective against treatment-naive CML stem cells from patients who subsequently proved to be resistant to IM therapy.

Conclusions Simultaneously targeting BCR-ABL and JAK2 activities in CML stem/progenitor cells may improve outcomes in patients destined to develop IM resistance.

J Natl Cancer Inst;2013;105:405–423

The defining hallmark of chronic myeloid leukemia (CML) is the *BCR-ABL* fusion gene originating in a hematopoietic stem cell (1–4). The BCR-ABL oncoprotein (p210$^{BCR-ABL}$) encoded by this gene displays constitutively elevated tyrosine kinase (TK) activity that drives the pathogenesis of the disease by perturbing multiple signaling pathways, including the RAS/MAPK, PI3K/AKT, and Janus kinase 2 (JAK2)/ signal transducer and activator of transcription 5 (STAT5) pathways (5,6). In particular, JAK2 physically interacts with the C-terminal region of BCR-ABL and is one of the most prominent targets of BCR-ABL (7,8). A recent study further suggests that the BCR-ABL–mediated signaling pathways in CML cells are controlled by JAK2 through direct phosphorylation of tyrosine 177 of BCR-ABL oncoprotein (9).

Imatinib mesylate (IM) and other BCR-ABL tyrosine kinase inhibitors (TKIs), including dasatinib (DA) and nilotinib (NL), have been introduced into clinical practice with remarkable therapeutic effects on chronic-phase (CP) CML (10–13). However, early relapses and the emergence of IM-resistant disease at any time can pose major setbacks for some patients (8,14,15), usually due to the selection and outgrowth of preexisting subclones of cells with mutations in the BCR-ABL kinase domain (14,16). Clinical evidence indicates that single agent, molecularly targeted therapies do not cure most patients, as molecular remissions are rare and disease frequently recurs when IM is discontinued, even after many years of treatment (17–20). Experimental studies have also shown that the most primitive CML cells are largely quiescent and innately insensitive to TKIs (21–27). Combination therapies to target other proteins or pathways, in addition to BCR-ABL, appear to be more effective at inhibiting these cells (28–31). Recent studies further suggest that survival and growth of primitive CML cells may not even depend on BCR-ABL–TK activity (32,33). We and others have demonstrated that leukemic stem cells (LSCs) possess multiple unique features expected to promote both their innate and acquired resistance to TKI therapies (16,24–27,34,35). Improved

treatment approaches to prevent the continuous development of resistant subclones by targeting other key molecular elements active in CML LSCs are thus clearly needed.

One candidate target is Abelson helper integration site 1 (*Abi-1/AHI-1*), an oncogene that is upregulated in CML LSCs, together with BCR-ABL (34,36,37). *Abi-1/AHI-1* encodes a unique protein with multiple SH3 binding sites, an SH3 domain, and seven WD40 repeats, all known mediators of protein–protein interactions (38). We previously demonstrated that overexpression of *Abi-1/AHI-1* in primitive hematopoietic cells gives them a growth advantage in vitro and the ability to generate leukemia in vivo, synergizing with *BCR-ABL* to enhance these outcomes (39). Conversely, stable suppression of *AHI-1* by small interfering RNA reduces the autonomous growth capability of very primitive CML cells and increases their response to TKIs in vitro. Importantly, AHI-1 physically interacts with BCR-ABL and JAK2 in CML cells to mediate these biological effects, although the nature of the direct or indirect interaction between AHI-1 and JAK2 still remains uncharacterized. We therefore hypothesized that a combination treatment strategy, designed to destabilize this new protein complex, might be a more effective approach to eliminating CML LSCs.

Materials and Methods

Retroviral and HA-Tagged Vectors and Virus Production

Abi-1 mutant constructs, including Ahi-1SH3$^{\Delta}$, Ahi-1SH3WD40$^{\Delta}$, and Ahi-1N-ter$^{\Delta}$, were polymerase chain reaction (PCR) amplified using a mouse stem cell virus (MSCV)–*Abi-1*–internal ribosomal entry site (IRES) –yellow fluorescent protein (YFP) vector containing full-length *Abi-1* cDNA as a template (39). The constructs were then subcloned into the MSCV–IRES–YFP retroviral vector using the HapI and XhoI sites. We also cloned them into a pcDNA3–human influenza hemagglutinin (HA) vector using its NotI and XbaI sites. Specific primers used are included in Supplementary Table 1 (available online). Constructs were verified by restriction enzyme digestion analysis and DNA sequencing.

Retrovirus production was performed as previously described (39). Briefly, retrovirus was obtained by transfecting ecotropic Phoenix packaging cells with each construct, and virus-containing supernatants were then used to transduce the murine pro-B cell line BaF3 and *BCR-ABL*–inducible BaF3 cells (40). YFP^{+} cells were then sorted by fluorescence-activated cell sorting (FACS). Several clonal cell lines per construct were selected. HA-tagged constructs were transfected into 293T cells by calcium phosphate precipitation and were then lysed and the proteins extracted for immunoprecipitation and Western blotting analyses.

Human Cells

Cells were obtained from newly diagnosed patients with CP CML before initiation of any TKI therapy. The clinical details of the patients from whom cells were obtained and their subsequent classification as IM responders or nonresponders, are given in Supplementary Table 2 (available online). Bone marrow (BM) cells were also obtained from healthy donors as leftover material from BM transplant harvests. Informed consent was obtained, and the procedures used were approved by the Research Ethics Board of the University of British Columbia and the University of Glasgow. CD34^{+} cells (>95% pure) were isolated immunomagnetically by positive selection of cells utilizing EasySep CD34 selection kits (STEMCELL Technologies, Vancouver, BC, Canada) or CliniMACS (Miltenyi Biotec, Auburn, CA). Purity was verified by restaining the isolated cells with a fluorescein-isothiocyanate (FITC)–labelled antihuman CD34 mouse monoclonal antibody (1:100 dilution) (STEMCELL Technologies) or with mouse monoclonal antihuman CD34 allophycocyanin (APC) (BD Biosciences, Mississauga, ON, Canada) (1:100 dilution) and analyzing the cells by FACS.

Reagents

TG101209 was provided by TargeGen Inc (San Diego, CA), reconstituted in dimethyl sulfoxide (Sigma-Aldrich, Oakville, ON, Canada) to 10 mM and stored at –20°C. IM and NL were obtained from Novartis (Basel, Switzerland) and stored at –20°C in 10 mM water and in dimethyl sulfoxide, respectively. DA was supplied by Bristol-Myers Squibb (Princeton, NJ), and a 10 mM stock solution of DA in dimethyl sulfoxide was stored at –20°C. An inhibitory concentration (IC_{50}) value for TG was determined based on the half maximal (50%) inhibitory concentration of TG on K562 cells using the trypan blue dye exclusion method. The IC_{50} value was also determined for CD34^{+} CML and normal BM cells incubated with four growth factors (20 ng/mL interleukin 3 [IL-3], provided by Novartis; 20 ng/mL interleukin 6 [IL-6], provided by Cangene, Mississauga, ON, Canada; 100 ng/mL Flt3-ligand, provided by Immunex, Seattle, WA; and 20 ng/mL granulocyte colony-stimulating factor [G-CSF], provided by STEMCELL Technologies).

Colony-Forming Cell and Long-Term Culture-Initiating Cell Assays

Colony-forming cell (CFC) assays were performed by plating CD34^{+} cells from CML patients (Supplementary Table 2, available online) in methylcellulose medium (supplemented with 20 ng/mL IL-3, 20 ng/mL IL-6, 20 ng/mL G-CSF, and 20 ng/mL granulocyte macrophage colony-stimulating factor (GM-CSF) (STEMCELL Technologies) with IM (5 μM), DA (150 nM), NL (5 μM), and TG101209 (TG) (100 nM), alone or in combination. In some experiments, CD34^{+} CML cells were cultured with drugs for 3 or 6 days before the remaining cells were washed and plated for CFC analysis.

For long-term culture-initiating cell (LTC-IC) assays, CD34^{+} CML cells were incubated with the same inhibitors in the presence of the four growth factors for 3 days. Untreated and inhibitor-treated cells were then overlaid on a preestablished, irradiated (M2-10B4) stromal cell layer in myeloid long-term culture medium (STEMCELL Technologies) supplemented with 10^{-6} M hydrocortisone, as previously described (41). Cultures were maintained for 5 weeks with weekly half-medium changes. Cells were then harvested and counted, and CFC assays were performed to obtain LTC-IC–derived CFC colonies as an indirect measure of the input LTC-IC number.

Cell Suspension Cultures and Viability Assays

CML cell lines (K562, K562 IMR, K562 lenti-AHI-1, K562 SH4-bulk, and BV173) were cultured in Roswell Park Memorial Institute 1640 media with 10% fetal bovine serum plus 100 U/mL penicillin

and 0.1 mg/mL streptomycin (STEMCELL Technologies). Parental and Ahi-1–transduced BaF3 cells were supplemented with 5 ng/mL murine IL-3 (STEMCELL Technologies). 293T cells and ecotropic packaging cells were grown in Dulbecco's modified Eagle's media with 10% fetal bovine serum, penicillin, streptomycin, and L-glutamine (STEMCELL Technologies). $CD34^+$ cells were cultured in Iscove's medium with bovine serum albumin, insulin, transferrin, low density lipoproteins (BIT; STEMCELL Technologies) and 10^{-4} M 2-mercaptoethanol. Cells were cultured with or without TKIs or TG alone or in combination with TG in the presence of four growth factors. For experiments lasting 6 days, cell were washed and resuspended in fresh drug on day 3. Total cell counts and viability was assessed using the trypan blue dye exclusion method.

Apoptosis Assays

Apoptosis analysis was performed using an Apoptosis Detection kit (BD Biosciences). Briefly, cells were stained with Annexin V phycoerythrin (PE) or FITC and 7-aminoactinomysin (7-AAD) (1:20 dilution) at 24, 48, and 72 hours for each test condition and analyzed using a FACSCalibur (BD Bioscience). Total apoptotic cell numbers were calculated as the sum of the "early" apoptotic cells (Annexin V^+ only) and "late" apoptotic cells (Annexin V^+/7-AAD^+). Phenotypic analysis of viable cells was performed by labeling cells with mouse monoclonal antihuman CD34 APC and mouse monoclonal antihuman CD38 PE antibodies (BD Bioscience) (1:100 dilution). Cells were considered positively stained if the level of fluorescence was above that of an isotype-matched control (BD Bioscience).

Quantitative Real-Time PCR Analysis

Total RNA was extracted using the Absolutely RNA Microprep kit (Stratagene, La Jolla, CA). Reverse transcription reactions and real-time PCR were performed using 25 µL of 2× SYBR Green PCR Master Mix (Applied Biosystems), 1 µL of 20 µM of specific primers, 1 to 2 µL cDNA, and water to a final volume of 50 µL. Specific primers to detect *BCR-ABL* transcripts were previously described (16).

Immunoprecipitation and Western Blot Analysis

Human cell lines (K562, K562 IMR, K562 lenti-AHI-1, and BV173) and murine cell lines (BaF3, BCR-ABL–inducible BaF3, and BaF3 cells overexpressing full length Ahi-1 and its mutant forms) were grown in complete Roswell Park Memorial Institute media. Cells were lysed in protein solubilization buffer, and protein concentration was determined as described previously (16). For immunoprecipitation, cell lysates were incubated with antibody at 4°C overnight (39). The immune complexes were incubated with protein G or protein A bead flurry for another 2 hours at 4°C. The samples were then heated at 70° C for 10 minutes and separated on 4% to 12% NuPAGE NOvex Bis-tris gradient gels (Invitrogen, Burlington, ON, Canada). Gels were transferred onto polyvinylidene difluoride membrane of 0.2 µm pore size (Millipore, Billerica, MA), and membranes were incubated with specific antibodies as described (16). The antibodies in this study included a rabbit polyclonal N-terminal AHI-1 antibody and an antimouse Ahi-1 mouse monoclonal antibody (1:1000 dilution) (C-mAhi-1 M5, Applied Biological Materials Inc Vancouver, BC, Canada), an antimouse ABL mouse monoclonal antibody (1:1000 dilution) (8E9; BD Biosciences), an antimouse JAK2 rabbit monoclonal antibody (1:1000 dilution) (Cell signaling Technology, MA), a rabbit polyclonal anti-JAK2 agarose conjugated antibody (Santa Cruz Biotechnology), anti-phospho-JAK2 rabbit polyclonal antibodies (1:1000 dilution) (Cell Signaling and Epitomics Inc, Burlingame, CA), an antihuman STAT5 rabbit polyclonal antibody (1:1000 dilution) (Millipore, Billeria, MA), an anti-phospho-STAT5 rabbit monoclonal antibody (1:1000 dilution) (Cell Signaling), an antihuman phospho-CRKL rabbit polyclonal antibody (1:2000 dilution) (Cell Signaling), an antihuman CRKL rabbit polyclonal antibody (1:1000 dilution) (Santa Cruz Biotechonolgy), an antiphosphotyrosine mouse monoclonal antibody (4G10) (1:2000 dilution) (Millipore, Billerica, MA), an anti-phospho-AKT rabbit polyclonal antibody (1:1000 dilution) (Cell Signaling), an antimouse Akt rabbit polyclonal antibody (1:1000 dilution) (Cell Signaling), an antihuman phospho-ERK rabbit polyclonal antibody (1:1000 dilution), an antirat ERK rabbit polyclonal (1:1000 dilution), an antimouse GAPDH mouse monoclonal antibody (1:2000 dilution) (Sigma Aldrich), an antiactin mouse monoclonal antibody (1:1000 dilution) (Sigma Aldrich), and an anti-HA mouse monoclonal antibody (1:1000 dilution) (Applied Biological Materials Inc). The antibody binding membranes were incubated with horseradish peroxidase–conjugated secondary antibody (1:5000 dilution) (Santa Cruz Biotechnology) for 1 hour at room temperature. The immunoreactive proteins were visualized by enhanced chemiluminescence.

CRKL and STAT5 Phosphorylation Assay by Intracellular Staining

After 24 and 72 hours, CML cells from each condition were stained with a 1:10 dilution of rabbit polyclonal P-CRKL (Tyr 207) and rabbit polyclonal P-STAT5 (Tyr 694) antibodies (New England Biolabs, Hitchin, UK) followed by incubation with a secondary goat antirabbit immunoglobulin G FITC–conjugated antibody (Sigma Chemicals) (1:50 dilution) before FACS analysis, according to a previously described protocol (42). The amount of P-CRKL and P-STAT5 in the sample were determined and expressed as a percentage of untreated controls.

Transplantation of Immunodeficient Mice With CML Cells

BV173 cells (2.5×10^6 input cells per treatment condition; n = 6 mice per group in two experiments) were cultured with or without 1 µM IM or 0.5 µM TG or both together for 3 days. $CD34^+$ CML cells (6×10^6 per treatment condition; n = 3 mice per group for each condition, per patient sample) from three CML samples were cultured in Iscove's minimum essential medium with 10% BIT, 1% L-glutamine, and four growth factors plus either 1µM IM or 100 nM TG or both or neither for 3 days. Recovered cells were then washed, and all cells recovered from each treatment group were injected intravenously into 8- to 10-week-old, sublethally irradiated (315 cGy) NOD/SCID–interleukin 2 receptor γ–chain-deficient (NSG) mice. The level of engraftment of BV173 cells in the BM was determined by labeling the cells with antihuman CD45 APC mouse monoclonal antibody (1:100 dilution), antihuman CD19 PE mouse monoclonal antibody (1:50 dilution), and antihuman CD20 PE mouse monoclonal antibody (1:50 dilution) (eBioscience, Canada) and analyzing by FACS. Mice were monitored weekly

for signs of weight loss or lethargy. For in vivo oral administration of TKIs or TG alone and in combination, BV173 cells (2.5×10^6 per mouse; n = 6 mice per group) were injected intravenously into 8- to 10-week-old, sublethally irradiated NSG mice. Two weeks posttransplantation, mice were treated with vehicle (oral administration of water), IM (50mg/kg), TG (60mg/kg), and IM (50mg/kg) plus TG (60mg/kg) twice a day for 2 weeks by oral gavage. Mice were monitored daily for body weight changes and survival during and after treatments.

To monitor human cell engraftment in mice injected with primary CD34$^+$ CML cells, BM cells were collected every 4 weeks by BM aspiration. Mice were then killed after 16 weeks, and BM cells were harvested from femurs, tibiae, and hip bones. Cells collected were labeled with antihuman CD45 FITC mouse monoclonal antibody (1:50 dilution), CD34 APC mouse monoclonal antibody (1:100 dilution), CD19/20 PE mouse monoclonal antibody (1:50 dilution), CD14/15/33/66b FITC mouse monoclonal antibodies (1:50 dilution), and CD3 APC mouse monoclonal antibody (1:100 dilution, BD Biosciences), and the percentage of human cells was determined by FACS analysis. To measure the proportion of *BCR-ABL*$^+$ human cells, *BCR-ABL* transcript levels in FACS-sorted human CD45$^+$ cells were evaluated by quantitative reverse-transcription PCR or fluorescence in situ hybridization. Animal experiments were performed in the Animal Resource Centre of the BC Cancer Agency Research Centre using procedures approved by the Animal Care Committee of the University of British Columbia (Vancouver).

Statistical Analysis

Results are shown as the mean value with 95% confidence intervals (CIs) obtained in triplicate independent experiments. Differences between groups were assessed using a two-sided Student *t* test for paired samples. Statistical analysis was also performed in some experiments using one way analysis of variance, with correction for multiple group comparison using GraphPad Prism version 5 (http://www.graphpad.com/prism/prism.htm). Methods appropriate to fitting linear mixed models were used to analyze the endpoints of proliferation over time, CFC output, and changes in P-STAT5 and P-CRKL. A *P* value less than .05 was considered statistically significant. For survival curve analysis, median durations of survival were presented, and log-rank tests were used to compare median survival of mice from different groups.

Results

Interaction of Ahi-1 With Jak2 and BCR-ABL via Different Binding Sites

To identify and characterize the functional domains of Ahi-1 that are critical for its interaction with Jak2 and/or BCR-ABL, we first generated several Ahi-1 mutants, including an N-terminal deletion mutant (Ahi-1N-ter$^\Delta$, containing both SH3 and WD40-repeat domains), an SH3 deletion mutant (Ahi-1SH3$^\Delta$), and a mutant in which both SH3 and the WD40 repeats were deleted (Ahi-1SH3WD40$^\Delta$) (Figure 1, A and C). We then stably transduced each of these mutants, or full-length *Ahi-1*, into BaF3 cells and *BCR-ABL*–inducible BaF3 cells (Figure 1A; Supplementary Figure 1A, available online; Supplementary Table 1, available online) (40). It was noticed that relatively higher levels of full-length Ahi-1 were found in *Ahi-1*–transduced BaF3 cells than in *BCR-ABL*–inducible cells cotransduced with *Ahi-1* (Figure 1A). Coimmunoprecipitation experiments revealed that Ahi-1 is highly expressed and stably associated with BCR-ABL in *BCR-ABL*–inducible cells cotransduced with full-length *Ahi-1* (Figure 1B, lower left panel, lane 5), consistent with our previous findings in human CML cells (39). Notably, Ahi-1 was detected in both *Ahi-1*–transduced BaF3 cells (without BCR-ABL), as well as in *BCR-ABL*–inducible cells, after immunoprecipitation with an anti-Jak2 antibody (Figure 1B, right panel, lanes 2 and 5). These experiments show that Ahi-1 can directly interact with Jak2 in a fashion that is independent of the presence of BCR-ABL. Moreover, in the same cells transduced with the Ahi-1N-ter$^\Delta$ mutant, a predicted 70-kD interaction product of Ahi-1 with Jak2 was not detectable (Figure 1B, right panel, lane 6), demonstrating a requirement for the N-terminal region of Ahi-1 for the Ahi-1–Jak2 interaction. Nevertheless, the Ahi-1–BCR-ABL complex could still be identified in these cells (Figure 1B, lower left panel, lane 6), indicating that the deleted N-terminal region of Ahi-1 is not required for its interaction with BCR-ABL. Epitope-tagged, full-length and mutant Ahi-1 constructs were then transiently expressed in 293T cells, with either BCR-ABL or Jak2, to test the reproducibility of these findings in another system (Supplementary Figure 1, B and C, available online). Analysis of the transduced 293T cells further showed that Ahi-1 mutants with deletion of either the SH3 domain only or both the SH3 and WD40-repeat domains together, but not the N-terminal region, did not interfere with Jak2 binding (Figure 1C, left panel). On the other hand, Ahi-1 molecules lacking the WD40-repeat domain lost the ability to bind to BCR-ABL, and the presence or absence of the adjacent SH3 domain did not affect this interaction (Figure 1C, right panel, lanes 2 and 4). Thus it can be concluded that the WD40-repeat domain is required for interaction of Ahi-1 with BCR-ABL, whereas the N-terminus of Ahi-1 is essential for its interaction with Jak2.

Effects of the Disruption of the Ahi-1–BCR-ABL–Jak2 Complex on IM Sensitivity of *BCR-ABL*$^+$ Cells

We next asked how altering the integrity of the Ahi-1–BCR-ABL–Jak2 complex would affect the ability of IM to induce apoptosis and inhibit proliferation of *BCR-ABL*$^+$ cells. To assess induction of apoptosis, *BCR-ABL*–inducible BaF3 cells transduced with full-length *Ahi-1* or its mutants were incubated for 24 hours in the presence or absence of IM, followed by determination of the frequency of Annexin V$^+$ cells. As expected, overexpression of full-length *Ahi-1* statistically significantly reduced the frequency of apoptotic cells induced by IM exposure (mean percentage of Annexin V$^+$ cell in *BCR-ABL*–inducible cells cotransduced with full-length *Ahi-1* vs *BCR-ABL*-inducible cells: 6.5% vs 27% in 2 μM IM, difference = 20.5%, 95% CI = 14.4% to 23.7%, $P < .001$; and 10% vs 34% in 5μM IM, difference = 28%, 95% CI = 21% to 36%, $P < .001$) (Figure 2, A). Strikingly, cells expressing the SH3WD40$^\Delta$ mutant displayed dramatically increased sensitivity to IM, with increased Annexin V$^+$ cells compared with *BCR-ABL*–inducible cells transduced with full-length *Ahi-1* (mean percentage of Annexin V$^+$ cells in Ahi-1 SH3WD40$^\Delta$ vs full-length Ahi-1: 64% vs 6.5% in 2 μM IM, difference = 53%, 95% CI = 49% to 57%, $P < .001$; and

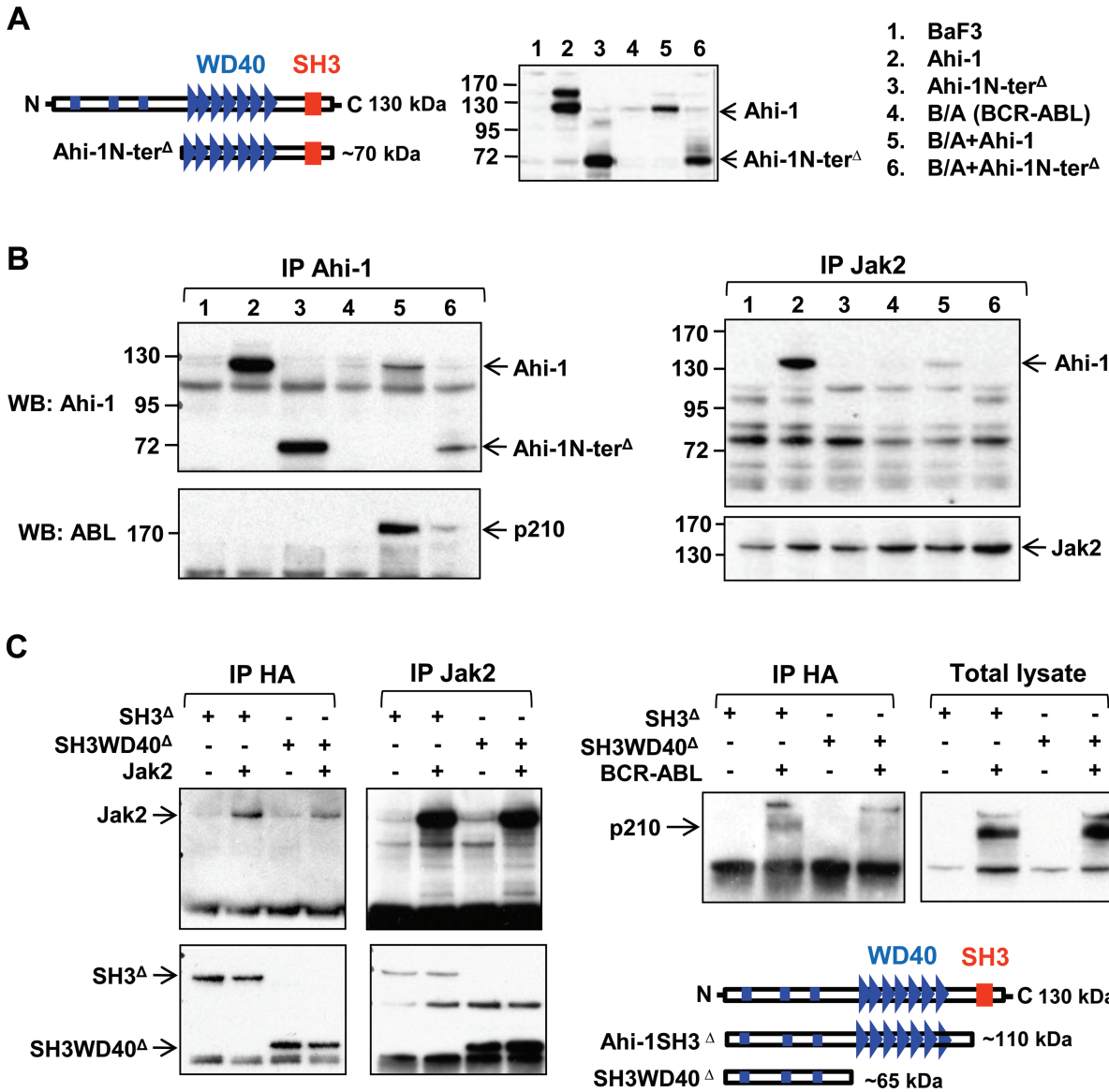

Figure 1. Evidence of Abelson helper integration site 1 (Ahi-1)–Janus kinase 2 (Jak2) and Ahi-1-BCR-ABL interactions in *BCR-ABL*– and *Jak2*-transduced cells coexpressing *Ahi-1* and its mutants. **A)** Schematic of functional domains of full-length and mutant (N-terΔ) Ahi-1. Vectors were transduced into BaF3 cells and *BCR-ABL*–inducible cells, and increased protein expression levels of full-length and mutant Ahi-1 were detected by Western blotting. **B)** Ahi-1 (**left panel**) or Jak2 (**right panel**) were immunoprecipitated from lysates of the same transduced cells and then electrophoresed and probed with specific antibodies, as indicated. **C)** Human influenza hemagglutinin (HA)–tagged SH3Δ or SH3WD40Δ mutants were transfected into 293T cells with or without a Jak2 vector, immunoprecipitated with antibodies to either HA or Jak2, electrophoresed, and probed using Jak2 or Ahi-1 antibodies (**left panel**). The **right panel** shows that these two mutants were coexpressed with *BCR-ABL*, immunoprecipitated with an anti-HA antibody, and probed with a c-ABL antibody. A schematic of the functional domains of full-length Ahi-1 and its SH3Δ and SH3WD40Δ mutants is below the right panel. IP = immunoprecipitation; WB = Western blotting.

69% to 10% in 5 μM IM, difference = 58%, 95% CI = 54% to 62%, $P < .001$); to a lesser extent, this was also seen in cells expressing the N-terΔ (17% vs 6.5% in 2 μM IM, difference = 8.9%, 95% CI = 5% to 13%, $P < .001$; 45% vs 10% in 5 μM IM, difference = 34.8%, 95% CI = 25.6% to 44%, $P < .001$) and the SH3Δ mutants (34% vs 6.5% in 2 μM IM, difference = 26.2%, 95% CI = 21.8% to 30.6%, $P < .001$; 42% vs 10% in 5 μM IM, difference = 31.6%, 95% CI = 26.8 % to 36.3%, I < .001) (Figure 2A; data not shown for cells in the presence of 5 μM IM). CFC assays performed with the same cells showed a statistically significantly reduced ability of *Ahi-1* mutants to form colonies in the absence of growth factors and presence of IM, with more statistically significant decreases in growth factor–independent colony growth from the SH3WD40Δ-transduced *BCR-ABL*–inducible cells, as compared with controls expressing full-length *Ahi-1* (mean CFC yields of Ahi-1N-terΔ vs full-length *Ahi-1*, 62% vs 108%, difference = 46%, 95% CI = 40% to 81%, $P < .001$; Ahi-1SH3Δ, difference = 61%, 95% CI = 33% to 60%, $P < .001$; Ahi-1SH3WD40Δ, difference = 102%, 95% CI = 90% to 115%, $P < .001$) (Figure 2B). Together, these results indicate a regulatory role for the Ahi-1 complex in the response/resistance of *BCR-ABL*$^+$ cells to IM, with the WD40-repeat and SH3 domains being directly involved in mediation of IM-induced apoptosis.

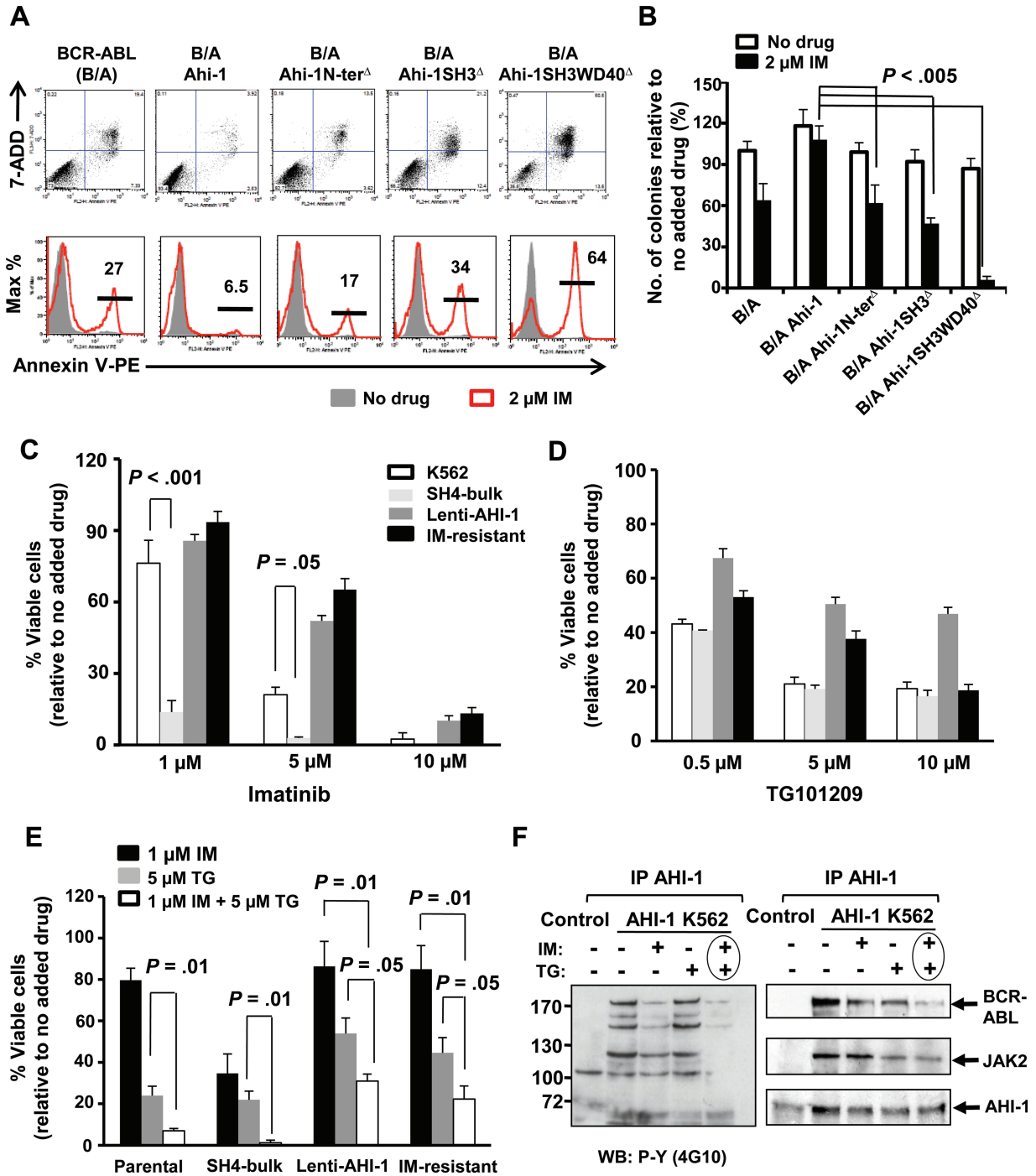

Figure 2. Effect of imatinib (IM) on induction of apoptosis and inhibition of colony formation in *BCR-ABL*–transduced cells coexpressing Abelson helper integration site 1 (*Ahi-1*) mutants and combined treatment with IM and a Janus kinase 2 (JAK2) inhibitor on inhibition of growth of *AHI-1*–overexpressing and IM-resistant cells. **A)** *BCR-ABL*–transduced cells coexpressing full-length *Ahi-1* and its mutants were cultured with IM, and the treated cells were stained with Annexin V/7-aminoactinomysin (7-AAD) to detect apoptotic cells after 24 or 48 hours. Representative fluorescence-activated cell sorting plots showing detection of Annexin V/7-AAD^{+} cells 24 hours after IM treatment are included. **B)** Transduced cells (200 cells/group) were pretreated with IM for 24 hours and then plated in colony-forming cell assays. Colony numbers produced in semisolid media were counted and expressed as a percentage of counts obtained from control cells without any drug added. **C–E)** Control K562 cells, *AHI-1*–transduced SH4-bulk K562 cells (with suppressed *AHI-1* expression), lenti-AHI-1 K652 cells (overexpressing *AHI-1*) and IM-resistant K562 cells were incubated with IM (**C**), or TG101209 (TG) alone (**D**), or both in combination (**E**), or with no drug for 48 hours and the percentage of viable cells was then measured. **F)** AHI-1 was immunoprecipitated from cell lysates of *AHI-1*–overexpressing K562 cells treated with IM and TG alone or in combination for 16 hours. The immunoprecipitates were then probed with an antityrosine phosphorylation antibody (4G10), a BCR-ABL antibody, a JAK2 antibody, and an AHI-1 antibody. Control cells = Hut78 cells. Data are means, and error bars represent 95% confidence intervals from three independent experiments in triplicate. *P* values were calculated using a two-sided Student *t* test. WB = Western blotting.

Viability of *AHI-1*–Overexpressing and IM-Resistant CML Cells Treated With IM and a JAK2 Inhibitor in Combination

We next asked whether targeting the AHI-1–BCR-ABL–JAK2 interaction complex by combining IM treatment with exposure to a selective JAK2 inhibitor, TG (43), could enhance the final inhibitory effects achievable with either agent alone. Treatment of *BCR-ABL*$^+$ K562 cells with graded doses of TG gave an IC_{50} value for these cells of 0.5 μM (Supplementary Figure 2A, available online). Western blot analysis revealed that the levels of P-JAK2 and P-STAT5 were greatly reduced in the presence of 5 μM after 4 hours, whereas total JAK2 and STAT5 protein expression was still unaffected (Supplementary Figure 2B, available online). TG alone also inhibited the growth of primary CD34$^+$ CML cells, with an IC_{50} value of 100 nM. Of note, CD34$^+$ normal BM cells were less sensitive to TG, with an IC_{50} value of 250 nM (Supplementary Figure 2A, available online).

Interestingly, K562 cells engineered to stably overexpress *AHI-1* (lenti-AHI-1) and IM-resistant K562 cells showed a reduced sensitivity to both IM (at 5 μM) and TG (at 0.5 and 5 μM), as assessed by a cell viability assay (Figure 2, C and D), but the results were not statistically significant. In contrast, K562 cells engineered to stably suppress *AHI-1* (SH4-bulk) showed a heightened sensitivity to IM at concentrations as low as 1 μM (percentage of viable cells in SH4 bulk cells vs control K562 cells: 13.8% vs 76.2%, difference = 62.4%, 95% CI = 30.7% to 60.2%, $P < .001$; 3.7% vs 19% at 5 μM IM, difference = 15.3%, 95% CI = 0.4% to 30.2%, P .05). However, IM together with TG was more effective at killing *AHI-1*–overexpressing cells (IM vs IM + TG: 82% vs 31%, difference = 53.3%, 95% CI = 25.5% to 85.2%, $P = .01$; TG vs IM + TG: 54% vs 31%, difference = 24%, 95% CI = 1.3% to 44.7%, $P = .05$) and IM-resistant K562 cells (IM vs IM + TG: 85% vs 22.3%, difference = 62.7%, 95% CI = 41.8% to 83.5%, $P = .01$; TG vs IM + TG: 44.7% vs 22.3%, difference = 22.3%, 95% CI = 0.8% to 45.4%, $P = .05$) (Figure 2E). IM-resistant cells also expressed higher levels of AHI-1 protein than the parental K562 cells (Figure 3A). Both parental and *AHI-1*–suppressed cells showed a significant increase in sensitivity to combination treatment compared with TG alone (TG vs IM + TG: 24% vs 7.1%, difference = 17%, 95% CI = 9.5% to 25%, $P = .01$, and 22% vs 1.2%, difference = 20.8%, 95% CI = 12.6 % to 29.1%, $P = .01$). Western blot experiments showed a biologically significant reduction in phosphorylation of CRKL, JAK2 and STAT5 in the *AHI-1*-overexpressing and IM-resistant K562 cells treated with IM plus TG, as compared to cells treated with IM or TG alone, while no change in phosphorylation of AKT and ERK was observed under the same conditions (Figure 3A). In addition, K562 cells and *AHI-1*–overexpressing cells treated either with TG alone or IM and TG together showed a marked reduction in AHI-1 and JAK2 protein expression. It was noticed that AHI-1 protein expression was only slightly reduced by the combination treatment in IM-resistant K562 cells, possibly due to activation of BCR-ABL–independent pathways, including persistently activated Lyn kinase, Fyn/ERK, and c-CBL, as previously reported (44–47). Moreover, the combination treatment was also more effective at reducing phosphorylation and protein expression of BCR-ABL, JAK2, and AHI-1 in BV173 cells as compared with cells treated with IM or TG alone (Figure 3B, right panel). Coimmunoprecipitation experiments further confirmed a stable complex of AHI-1–BCR-ABL–JAK2 in *AHI-1*–overexpressing K562 cells after immunoprecipitation with an anti-AHI-1 antibody (Figure 2F). Importantly, this protein interaction complex was markedly interrupted in the same cells treated with IM plus TG, as compared with cells treated with IM or TG alone. This resulted not only in a marked reduction in phosphorylation of BCR-ABL (Figure 2F, left panel), but also in reduction in protein expression of BCR-ABL, JAK2, and AHI-1 (Figure 2F, right panel). These results indicate that simultaneous treatment of *BCR-ABL*$^+$ cells with IM and a JAK2 inhibitor destabilizes, and hence downregulates, the activity of the AHI-1–BCR-ABL–JAK2 complex, leading to enhanced death of *AHI-1*–overexpressing and IM-resistant *BCR-ABL*$^+$ cells.

Effects of TG in Combination With TKIs on Very Primitive CML Patient Cell Survival

To determine whether the effects obtained using a combined BCR-ABL–JAK2 targeting approach on cell lines would extend to primary CP CML cells, we isolated *BCR-ABL*$^+$CD34$^+$ cells from three patients' samples obtained at diagnosis and then cultured these cells in liquid suspension with growth factors for 3 days in the presence of 5 μM IM, 5 μM NL, 150 nM DA, or 100 nM TG alone or in combination with TG. As expected, the percentages of viable cells present in cultures containing a single TKI or TG were lower than the values measured in the corresponding cultures to which no drug was added (TG, 38.1%, difference = 61.9%, 95% CI = 37.7% to 86.1%, $P < .001$; IM, 55%, difference = 48%, 95% CI = 23.8% to 72.2%, $P < .001$; NL, 42.3%, difference = 57.7%, 95% CI = 33.5% to 81.8%, $P < .001$: DA, 45.6%, difference = 54.4%, 95% CI = 30.2% to 78.6%, $P < .001$) (Figure 4A, left panel). However, the addition of TG to any TKI (regardless of the TKI type) resulted in a progressive reduction in the expansion of viable cells compared with TKI-only treated arms, with a clear dependence of the effect of the addition of TG over time (test for time–TG interaction, $P < .001$); the estimated relative reduction was 7% at 24 hours (95% CI = −12% to 22%), 13% at 48 hours (95% CI = −5% to 27%) and 49% at 72 hours (95% CI = 38% to 57%) (Figure 4A, right panel). No substantial toxic effects were observed in CD34$^+$ cells from three normal individuals treated with TKI and TG alone or in combination during equivalent cultures (Figure 4A, lower panels). Assessment of viability by Annexin V staining provided a more sensitive measure of the induction of apoptosis, with statistically significant differences apparent when comparing TG plus a TKI in combination with each single agent TKI treatment (IM vs IM + TG: 15.2% vs 40.5%, difference = 25.3%, 95% CI = 10% to 40.7%, $P < .001$; NL vs NL + TG: 19.5% vs 44.1%, difference = 24.65%, 95% CI = 9.3 % to 40%, $P < .001$; DA vs DA + TG: 17.2% vs 51.6%, difference = 34.3%, 95% CI = 19% to 49.6%, $P < .001$) (Figure 4B, left panel). These effects were not observed in CD34$^+$ normal BM cells with the same treatments, including the combination treatments (Figure 4B, right panel). We also analyzed the CD34$^+$CD38$^+$ and CD34$^+$CD38$^{-/low}$ subsets present in these 3-day cultures. Single agent treatments caused a reduction in the number of more-mature CD34$^+$38$^+$ progenitor cells, but more-primitive 34$^+$38^{low} cells (a population with higher short-term expansion potential) and 34$^+$38$^-$ cells (a stem cell–enriched population) were less sensitive to these agents alone (twofold and threefold fewer

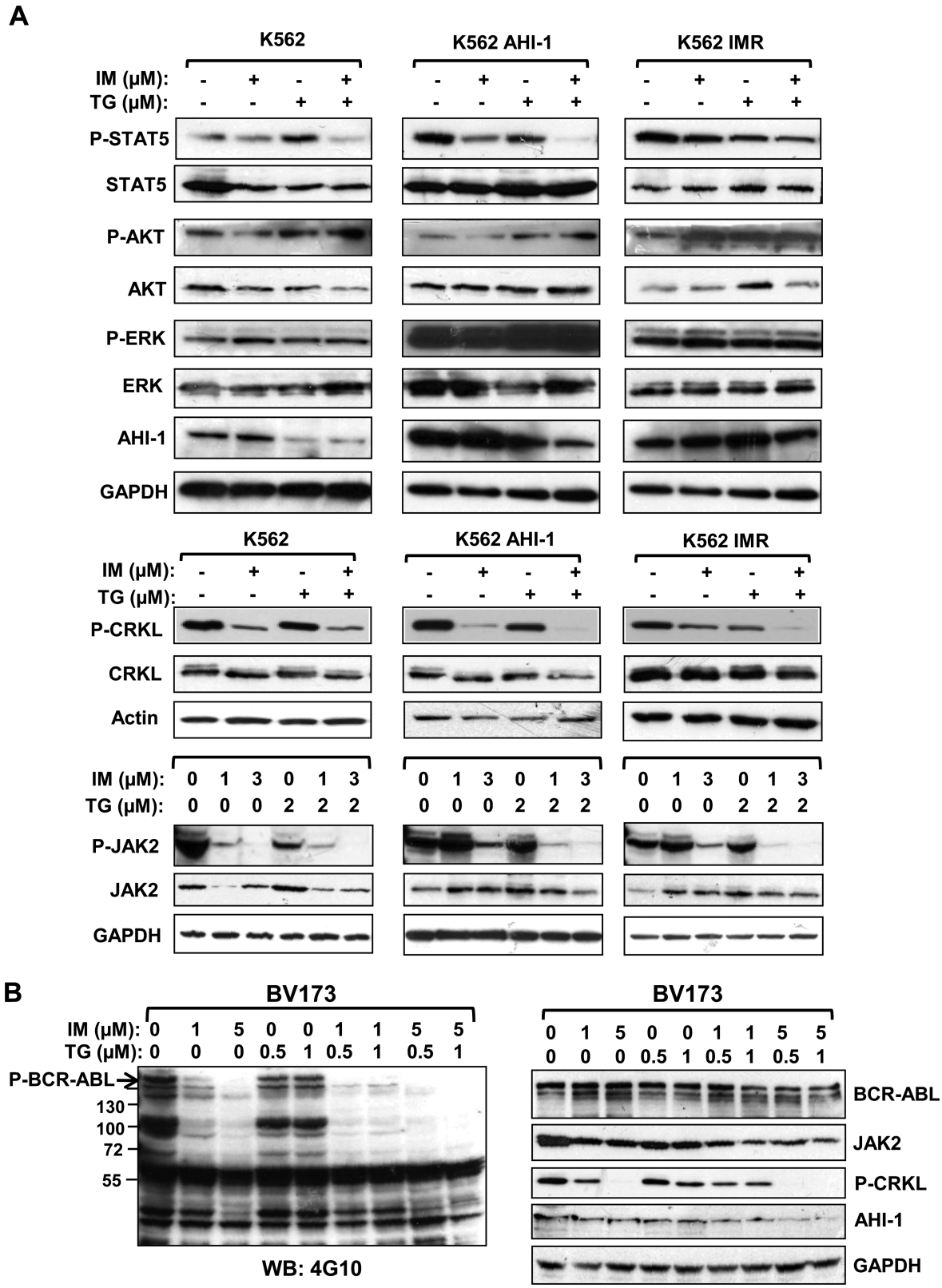

Figure 3. Inhibition of phosphorylation of BCR-ABL, CRK-like (CRKL), Janus kinase 2 (JAK2), and signal transducer and activator of transcription 5 (STAT5) in transduced K562 cells in response to combined treatment with TG101209 (TG) and imatinib (IM). **A)** K562 cells, Abelson helper integration site 1 (*AHI-1*)–overexpressing K562 cells, and IM-resistant K562 cells (IMR) were cultured with or without IM, TG, or a combination of IM and TG for 16 hours. Western blot analysis detected phosphorylation and protein expression of various proteins using the specific antibodies indicated. **B)** BV173 cells were treated with IM, TG, or IM plus TG for 16 hours. Cell lysates were immuno-probed with the specific antibodies indicated. GAPDH or actin was utilized as a loading control.

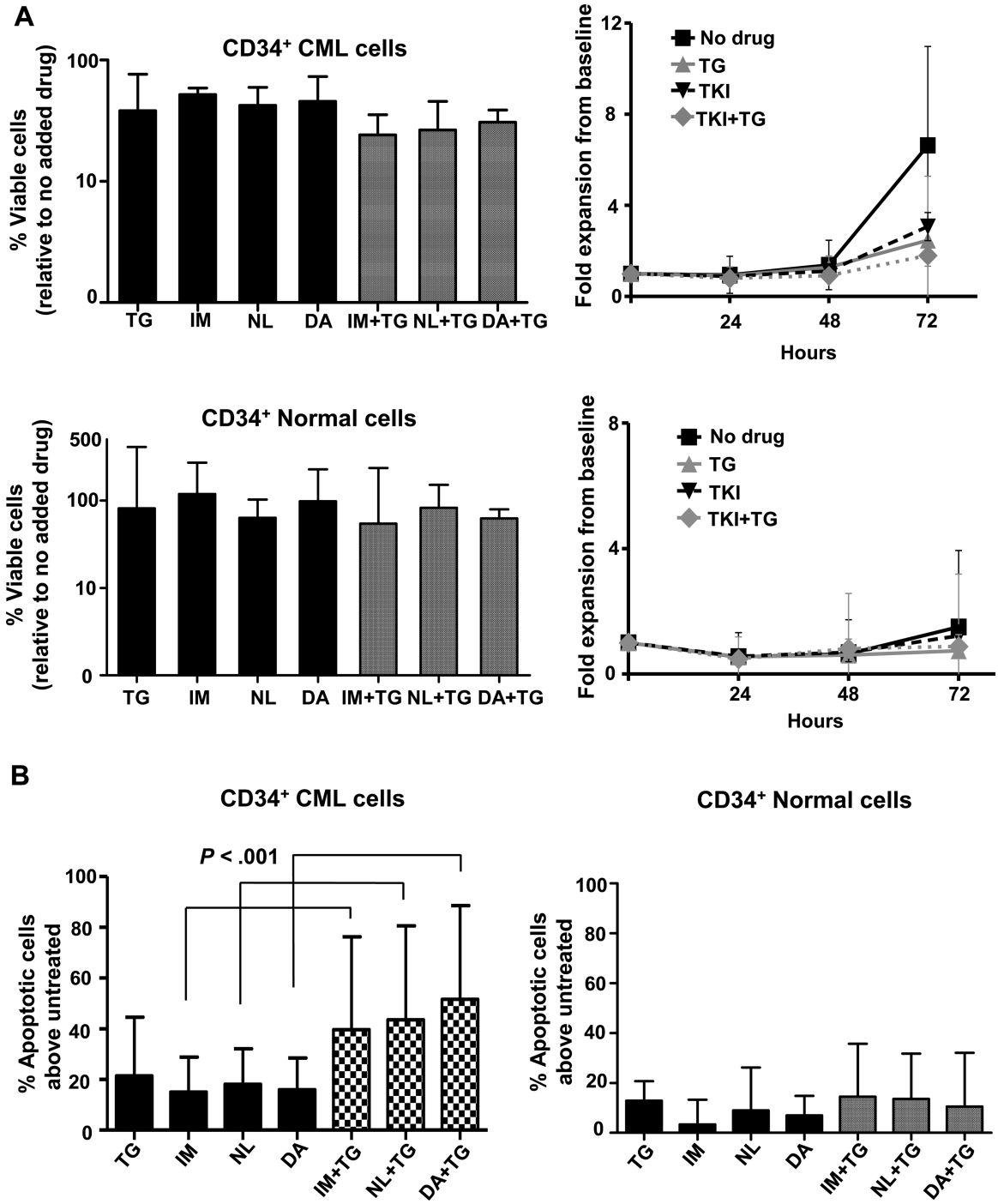

Figure 4. Effects of TG101209 (TG) in combination with tyrosine kinase inhibitors (TKIs) on the viability and induction of apoptosis in primary CD34+ chronic myeloid leukemia (CML) cells. **A)** CD34+ CML cells (n = 3, **upper left panel**) and CD34+ normal bone marrow (BM) cells (n=3, **lower left panel**) were analyzed after 72 hours of drug exposure (**solid bars** = no added drug; **checkered bars** = drug added). Viable cell frequencies were assessed by counting trypan dye–excluding cells. These were then expressed as a percentage of the frequency of viable cells in parallel cultures to which no drug was added (**left panel**) or used to calculate the total content of viable cells in the culture (**right panel**). **B)** Percentage of total apoptotic cells after 72 hours of drug treatment of CD34+ CML cells (n = 3) and normal BM cells (n = 3) determined by Annexin V/7-aminoactinomysin (7-AAD) staining. *P* values were calculated using one-way analysis of variance with correction for multiple group comparison for individual treatment arms (**B**). Data are means, and error bars represent 95% confidence intervals of triplicate measurements. NL = nilotinib; DA = dasatinib.

cells in cultures with TKIs or TG, respectively, as compared with untreated controls after 3 days in culture). This is consistent with our previous observations that more-primitive CML cells were less sensitive to TKI treatment than their more-mature cells (33,48). However, combination treatment with TKI and TG reduced the numbers of the $34^{+}38^{low}$ cells compared with either of the single agents alone and, more strikingly, caused an absolute reduction in the number of $34^{+}38^{-}$ cells (>10-fold reduction) (Figure 5A). These

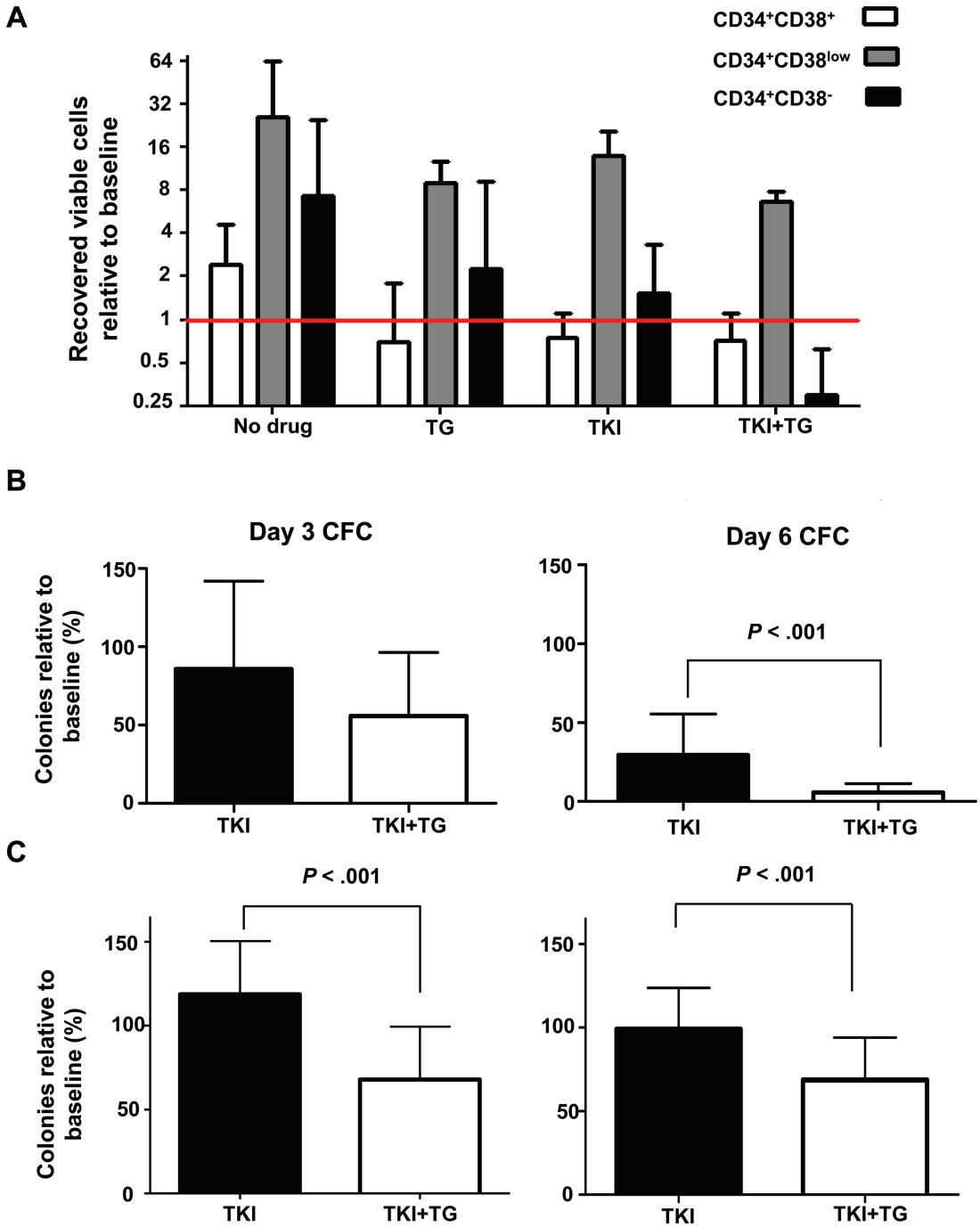

Figure 5. Effects of TG101209 (TG) in combination with tyrosine kinase inhibitors (TKIs) on multiple subsets of CD34+ chronic myeloid leukemia (CML) cells. **A)** CD34+ CML cells (n = 3) were cultured for 72 hours in the presence of imatinib (IM), nilotinib (NL), dasatinib (DA), or TG alone or a combination of TKI with TG, and the phenotypes of cells present within the viable (AnnexinV-/7-aminoactinomysin [7-AAD-]) gate were then determined by fluorescence-activated cell sorting based on their expression of CD34 and CD38. The total number of viable cells within each subpopulation was then calculated based on viable cell counts at 72 hours and compared with the starting number of cells within each subpopulation (baseline), represented by the **red line**. **B–C)** CD34+ CML cells (n = 2) (**B**) from newly diagnosed chronic-phase patients and CD34+ normal bone marrow (n = 3) (**C**) were plated in standard colony-forming cell (CFC) assays after 3 (**left**) or 6 (**right**) days of prior incubation in suspension cultures with 5 μM IM, 150 nM DA, 5 μM NL, or 100 nM TG alone or in combination. Colonies produced in the CFC assays were counted after 12 to 14 days of further incubation, and the numbers obtained are expressed as a percentage of values obtained in control assays without drug added. Data are means, and error bars represent 95% confidence intervals of triplicate measurements. *P* values were calculated using methods appropriate to fitting linear mixed models.

results suggest that combining TKI with TG has a more potent effect on the most primitive stem cell compartment.

Next we asked whether the combination of TG plus a TKI could also target primary CML CFCs. We first incubated CD34+ CML cells with TKIs alone, or with TG plus a TKI, for 3 or 6 days. An aliquot was then plated in growth factor–supplemented methylcellulose medium to determine the number of CFCs present. After a 3-day exposure, a 37% relative reduction of the CFC recovered

with TKI alone was recorded when TG was added to TKI (95% CI= –24% to 68%, $P = .18$). However, after a 6-day exposure, this increased to 86% (95% CI = 72% to 93%, $P < .001$), with a clear dependence of the effect of the addition of TG over time (test for time–TG interaction, $P = .003$) (Figure 5B). A toxic effect on CFC output of CD34$^+$ normal BM cells was noted when adding TG to TKI. The magnitude of this effect was similar to that seen on CML CD34$^+$ cells after 3 days, but importantly was not enhanced over time, with no further reduction in the number of colonies observed in the combination arm after 6 days of culture (44% relative reduction (95% CI = 29% to 56%, $P < .001$; test for time–TG interaction, $P = .19$) (Figure 5C). These results indicate that TKI plus TG is more effective at eliminating primary CML stem/progenitor cells than single TKIs, including cells that generate CML CFCs in short-term cultures; this effect is enhanced over time. Moreover, using a carefully selected concentration of TG, only a moderate toxic effect on normal BM was observed, which did not increase over time, thus providing a therapeutic window for the combination arm.

Elimination of Treatment-Naive CML Stem/Progenitor Cells From Clinically Defined IM Nonresponder Patients Using TG in Combination With a TKI

To determine whether simultaneously targeting both BCR-ABL and JAK2 activities could be therapeutically effective for CP patients who do not respond adequately to treatment with a single TKI, we investigated CML cells obtained at diagnosis from four CP patients who were classified retrospectively, after initiation of IM therapy, as clinical nonresponders (Supplementary Table 2, available online). The number of CFC colonies obtained in cultures containing TG or TKIs alone was reduced from the control value by less than 50% (Figure 6A), as expected (49). However, when TG plus a TKI was present, a statistically significant greater reduction in colony formation was seen (mean CFC yields of IM vs IM + TG: 54% vs 16%, difference = 39%, 95% CI = 35% to 68%, $P < .001$; DA vs DA + TG: 44% vs 11%, difference = 33%, 95% CI = 33% to 64%, $P < .001$; NL vs NL + TG: 59% vs 17%, difference = 43%, 95% CI = 30% to 65%, $P < .001$) (Figure 6A, left panel). It was interesting to note that treatment with a combination of TKIs, IM plus DA or IM with NL, was not effective at reducing CFC numbers from IM nonresponders. To assess effects on more primitive LTC-ICs, we incubated the initially isolated CD34$^+$ cells for 3 days in suspension culture, with growth factors and TG or TKIs alone or in combination, and then harvested the cells and plated equal aliquots in LTC-IC assays. The CFC outputs obtained 5 weeks later showed even less evidence of an effect of single-agent treatment on the LTC-IC numbers present in the 3-day cultures (Figure 6B). However, a statistically significant reduction in LTC-IC–derived colony yields was obtained with any of the combination treatments (mean LTC-IC–derived CFCs of IM vs IM + TG: 72% vs 26%, difference = 46%, 95% CI = 32% to 65%, $P < .001$; DA vs DA + TG: 59% vs 18%, difference = 40%, 95% CI = 30% to 69%, $P < .001$; NL vs NL + TG: 62% vs 22%, difference = 41%, 95% CI = 35% to 68%, $P < .001$). Importantly, toxic effects were not observed in experiments initiated with CD34$^+$ cells from normal individuals (Supplementary Figure 3A, available online). These results indicate that combination treatment with TKI and TG is effective at targeting very primitive CML stem/progenitor cells from IM nonresponders before they display evidence of resistance.

Effects of Combined Exposure of CD34$^+$ CML Cells to TG and a TKI on Suppression of BCR-ABL and JAK2/STAT5 Activities

We then examined changes in the phosphorylation of CRKL and STAT5, as indicators of BCR-ABL kinase activity. P-STAT5 is also activated by JAK2 kinase and can therefore be used as a measure of JAK2 kinase activity. The levels of phosphorylation of P-CRKL and P-STAT5 were analyzed in CD34$^+$ cells isolated from three CML samples after 24 hours incubation with no drug, or TG or one of the three TKIs alone, or in combination. We found that the levels of P-STAT5 were statistically significantly reduced upon addition of TG to TKI when compared with TKI treatment alone (35% relative reduction, 95% CI = 12% to 53%, $P < .001$), whereas the reduction in P-CRKL levels was marginally non-statistically significant (20% absolute reduction in phosphorylation rates [expressed as a percentage of baseline], 95% CI = –4% to 45%, $P = .11$). These combination effects were enhanced following another 48 hours of drug exposure, demonstrating the dependence of the effect of the addition of TG on time (P-CRKL: 60% absolute reduction in phosphorylation rates [expressed as a percentage of baseline], 95% CI = 35% to 84%, $P < .001$; and P-STAT5: 55%, 95% CI = 39% to 67%, $P < .001$). The respective tests for TG dependence on time are statistically significant for both P-CRKL ($P = .03$) and P-STAT5 ($P = .03$) (Figure 6C). Addition of TG to TKI treatment also caused a reduction in P-STAT5 levels after 24 hours in normal CD34$^+$ cells, which express relatively low levels of P-STAT5. However this reduction was not as great as that observed in CML CD34$^+$ cells in equivalent cultures (21% relative reduction compared with TKI, CI = 9% to 31%, $P = .004$) (Supplementary Figure 3B, available online). These results indicate that combined TG and TKI treatment markedly and durably inhibits the activity of BCR-ABL and JAK2 in CML stem/progenitor cells and to a higher degree than in normal cells.

Survival of Leukemic Mice Treated With TG and IM

To more definitively test the ability of TG in combination with a TKI (IM) to eliminate CML cells with in vivo leukemia propagating activity, we first undertook an experiment in which BV173 cells were exposed to these drugs for 3 days in vitro and then assayed posttreatment for their ability to produce leukemic progeny in NOD/SCID–interleukin 2 receptor γ–chain-deficient (NSG) mice. BV173 cells (derived from a BM sample of a CML blast crisis patient), but not K562 cells, have been shown to generate a lethal leukemia in NOD/SCID mice (50), and NSG mice are even more permissive to repopulation by leukemic cells, compared with normal human hematopoietic cells (51). Accordingly, 2.5×10^6 BV173 cells were cultured with or without 1 μM IM alone, 0.5 μM TG alone, or IM plus TG at the same concentrations for 3 days, followed by injection of all of the cells present at that time (ie, all of the progeny derived from the 2.5×10^6 input cells) into sublethally irradiated NSG mice (n = 6 mice per condition). Three weeks later, there were no statistically significant differences in the frequency of human *BCR-ABL*$^+$CD19/CD20$^+$ (BV173) cells in the BM of mice transplanted with IM- or TG-pretreated cells, as compared with

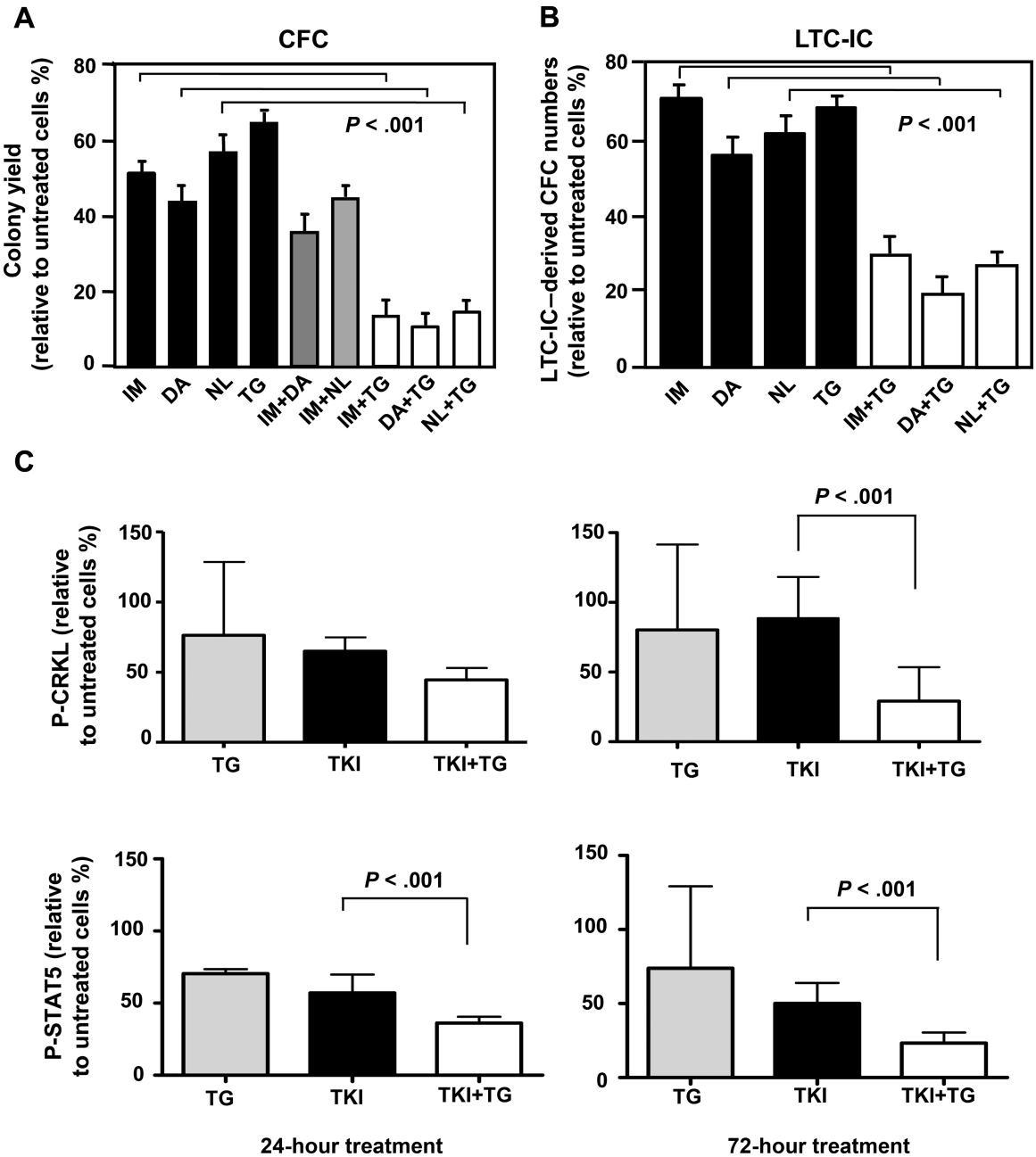

Figure 6. Proliferation of primitive chronic myeloid leukemia (CML) cells from clinically tyrosine kinase inhibitors (TKI)–resistant patients and CRK-like (CRKL) and signal transducer and activator of transcription 5 (STAT5) phosphorylation in these cells in response to combination treatment with TG101209 (TG) and TKI. **A)** $CD34^+$ CML cells from four newly diagnosed chronic-phase patients, subsequently classified clinically as imatinib (IM) nonresponders, were plated in standard colony-forming cell (CFC) assays plus 5 μM IM, 150 nM dasatinib (DA), 5 μM nilotinib (NL), or 100 nM TG alone or in combination. Colonies produced were counted after 12 to 14 days of incubation, and the numbers obtained were expressed as a percentage of values obtained in control assays to which no drugs were added. **B)** $CD34^+$ CML cells from three patients studied in (**A**) were incubated for 3 days in suspension cultures with 5 μM IM, 150 nM DA, 5 μM NL, or 100 nM TG alone or in combination and then assayed for long term culture-initiating cells (LTC-ICs). LTC-IC–derived CFC values were derived from the LTCs harvested 5 weeks later and then expressed as a percentage of the LTC-IC CFC numbers obtained for cells initially incubated for 3 days in the absence of any added drug. **C)** Phosphorylation of CRKL (**upper panels**) and STAT5 (**lower panels**) in $CD34^+$ CML cells (n = 3) was measured by fluorescence-activated cell sorting after 24 and 72 hours of drug exposure and expressed as a percentage of cells incubated for the same time in the absence of any drug. Data are means, and error bars represent 95% confidence intervals from three independent experiments in triplicate. *P* values were calculated using a two-sided Student *t* test (**A** and **B**) or methods appropriate to fitting linear mixed models (**C**).

recipients of control cells (incubated for 3 days without any drug) (Figure 7A). However, by comparison, the BM of mice injected with cells that had been exposed to IM and TG in combination contained fewer human $CD19/CD20^+$ cells (0.04% compared with 18% from untreated control cells, 6.2% for IM alone, and 15% for TG alone). We observed that mice injected with untreated cells died within 53 days, demonstrating the relatively aggressive nature of this CML model. A trend toward prolonged survival was observed in mice injected with the TG- plus IM-treated cells, but this differential effect did not achieve statistical significance (data not shown).

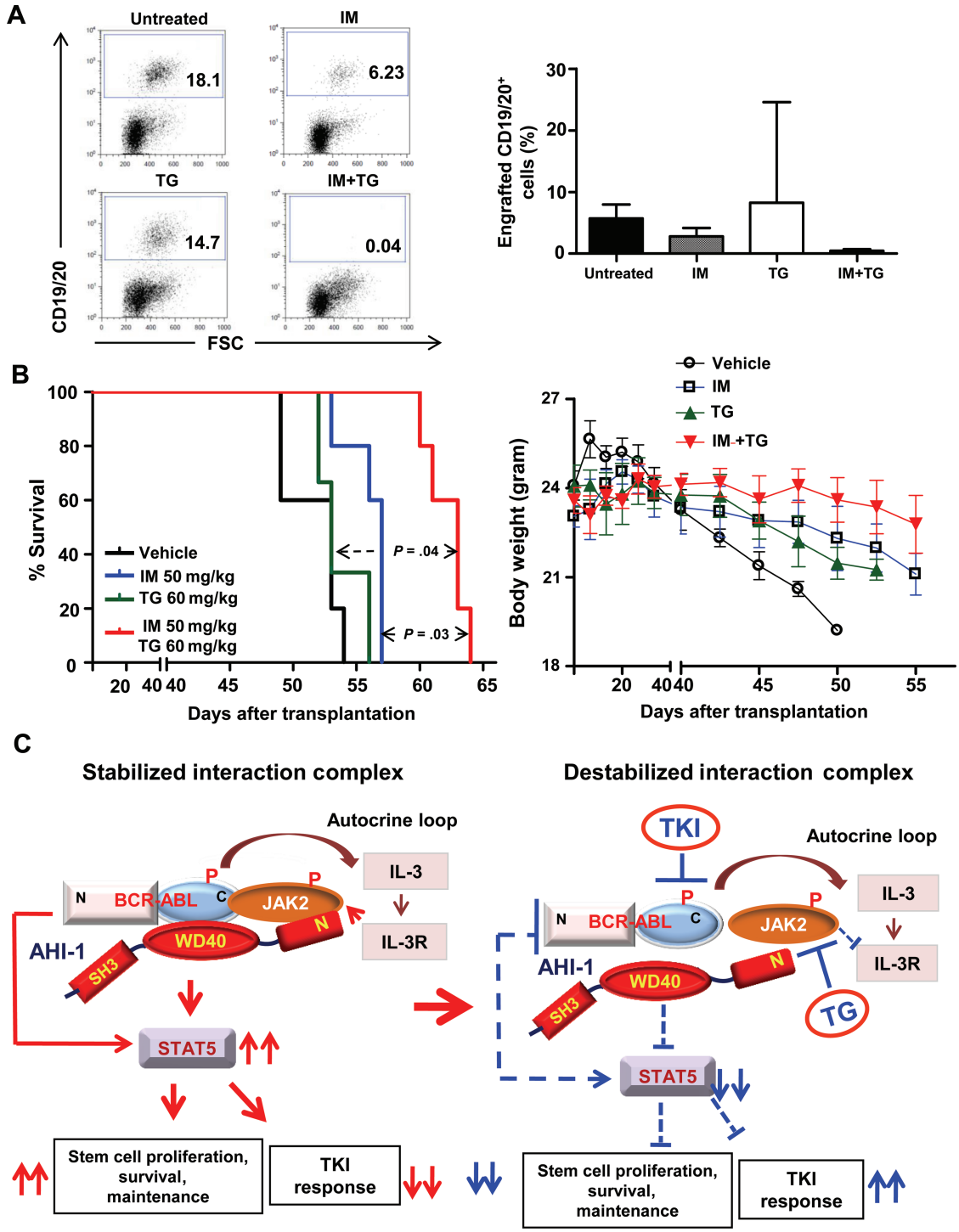

Figure 7. Effects of oral administration of TG101209 (TG) and imatinib (IM) on elimination of chronic myeloid leukemia (CML) BV173 cells and survival of leukemic mice in immunodeficient mice. **A)** BV173 cells were cultured with 1.0 μM IM, 0.5 μM TG, IM plus TG, or no drug for 3 days, and the progeny recovered from 2.5×10^6 initial cells were then injected intravenously into NOD/SCID–interleukin 2 receptor γ–chain-deficient (NSG) mice (n = 6 mice per condition). The **left panel** shows fluorescence-activated cell sorting profiles of engrafted human CD19/20+ cells detected in bone marrow aspirates of representative mice obtained 3 weeks posttransplant. The percentage of human CD19/20+ BV173 cells detected in the bone marrow of mice examined 3 weeks after injection is shown in the **right panel**. Data are means, and error bars represent 95% confidence intervals of six measurements per condition. **B)** Survival curve for recipients of BV173 cells (2.5×10^6 per mouse; n = 6 mice per group) treated by oral gavage beginning at 2 weeks posttransplant with vehicle, IM (50mg/kg), TG (60mg/kg), and IM (50mg/kg) plus TG (60mg/kg) twice a day for 2 weeks. Statistically significantly prolonged survival was observed in mice receiving the combination treatment (**left panel**). Body weights of mice in each treated group were measured, as indicated in the **right panel**. Log-rank tests were used to compare median survival of different groups (n = 6 mice per group), and *P* values were calculated using a two-sided Student *t* test. **C)** Model of the mechanism by which Abelson helper integration site 1 (AHI-1)–BCR-ABL and AHI-1–Janus kinase 2 (JAK2) interactions regulate constitutive activation of BCR-ABL and JAK2/ signal transducer and activator of transcription 5 (STAT5), resulting in increased leukemic stem cell proliferation, survival and maintenance and reduced tyrosine kinase inhibitor (TKI) response of these cells. Targeting both BCR-ABL and JAK2 activities to destabilize this complex perturbs these biological properties. IL-3 = interleukin 3; IL-3R = interleukin 3 receptor.

To improve the in vivo treatment effect in this aggressive CML model system, we assessed an oral treatment approach. The same numbers of BV173 cells (2.5×10^6) were injected into NSG mice. After about 2 weeks, mice were given oral gavage treatment with IM monotherapy (50 mg/kg), TG monotherapy (60 mg/kg), or IM plus TG combination therapy twice a day for 2 weeks (n = 6 mice per condition, including vehicle control). Interestingly, we observed statistically significantly prolonged survival in mice treated with the combination as compared with mice treated with TG or IM alone (median survival of IM + TG vs untreated: 63 days vs 53 days, ratio = 0.84, 95% CI = 0.56 to 1.1, $P = .002$; TG: 53 days, ratio = 0.84, 95% CI = 0.6 to 1.1, $P = .004$; IM: 57 days, ratio = 0.9, 95% CI = 0.61 to 1.2, $P = .003$) (Figure 7B, left panel). In addition, mice treated with the combination showed a reduction in weight loss compared with mice treated with single agents (Figure 7B, right panel). These results indicate that the oral combination treatment is more effective than either alone in eliminating human CML cells that are capable of generating an aggressive leukemia in mice, with statistically significant enhanced survival of leukemic mice.

Effects of the Combination of TG Plus IM on CML LSCs With In Vivo Leukemia-Initiating Activity

We then undertook additional experiments to determine the effect of combined TG plus IM treatment on the subsequent in vivo leukemogenic activity of primary CP CML cells transplanted into NSG mice. $CD34^+$ CML cells (6×10^6 per treatment condition) from three CML patients who were subsequently classified as nonresponders after IM therapy were exposed to 1.0 μM IM, 100 nM TG, or both together for 3 days. The cells recovered from the 3-day drug exposure cultures were then injected into sublethally irradiated NSG mice (n = 3 mice per group for each patient sample). IM plus TG treatment of primary $CD34^+$ CML cells in vitro greatly reduced the levels of human $CD45^+$ and $CD34^+$ leukemic cells regenerated in the BM of transplanted NSG mice, as measured for 16 weeks, compared with cells pretreated with IM or TG alone (Figure 8A). Engrafted myeloid cells ($CD14^+CD15^+CD33^+CD66b^+$) appeared to be reduced to a greater extent in the BM of mice treated with the drug combination, as compared with single-agent treatments (0.7% vs 2.2 to 3.6%) (Figure 8, B and C), and $CD34^+$ cells, in particular, were almost undetectable in the BM of mice injected with cells that had been pretreated with the TG plus IM combination at 16 weeks (Figure 8A, lower panel). Quantitative reverse-transcription PCR analysis further demonstrated statistically significant reductions in *BCR-ABL* transcript levels in FACS-purified $CD45^+$ BM cells of mice injected with CML cells treated with the combination of TG plus IM, as compared with mice injected with the same patients' cells pretreated with IM or TG alone or maintained in a medium without either agent (*BCR-ABL* transcript levels measured at 4 weeks, IM vs IM + TG (undetectable): 0.76 vs 0, difference = 0.76, 95% CI = 0.64 to 0.84, $P < .001$; TG, 0.53, difference = 0.53, 95% CI = 0.34 to 0.7, $P < .001$; at 12 weeks, IM vs IM + TG = 7.8 vs 0.3, difference= 7.5, 95% CI = 5.9 to 9.1, $P < .001$) (Figure 8D). Notably, *BCR-ABL* transcripts were increased in mice treated with IM at 12 weeks, indicating a lack of a biologically significant effect on the LSCs. Fluorescence in situ hybridization analysis confirmed that more than 90% of the human cells obtained from mice transplanted with CML cells not exposed to drug were *BCR-ABL*$^+$. These results show that the combined treatment with IM plus TG more effectively eliminates CML LSCs than IM or TG alone.

Discussion

In this study, we provide new evidence for AHI-1's role in mediating TKI response of CML cells by identifying independent AHI-1–JAK2 and AHI-1–BCR-ABL interactions that directly link these two kinases and AHI-1 in CML cells. Specifically, we show that loss of the ability of AHI-1 to interact with BCR-ABL, via its WD40-repeat and SH3 domains, substantailly enhances the apoptotic response and inhibits proliferation of *BCR-ABL*$^+$ cells exposed to TKIs (Figure 2). These findings provide a molecular mechanism to explain our previous observation that full-length *Abi-1/AHI-1* mediates both the transforming activity of *BCR-ABL* in primitive hematopoietic cells and the IM resistance characteristics of CML stem/progenitor cells through activation of the BCR-ABL and JAK2/STAT5 pathway (39). A number of recent studies of other WD40-repeat–containing scaffold proteins (52,53) reinforce the concept that AHI-1 serves as a regulator of the TK activity of both BCR-ABL and JAK2. For example, MORG1, a binding partner of the ERK pathway scaffold protein MP1, interacts with multiple components of the ERK cascade (MP1, Raf-1, MEK1, MEK2, ERK1, and ERK2) to stabilize their assembly into an oligomeric complex that regulates numerous cellular functions in normal and cancerous cells (52). RACK1, another WD40-containing protein, interacts with ABL only in transformed cells, and the introduction of RAS enhances this association of RACK1 with ABL, mediating altered signaling activities (54). In addition, truncating mutations that delete the WD40-repeat and SH3 domains of AHI-1 underlie Joubert syndrome (55,56), a disease that may be mediated by an AHI-1 and HAP1 molecular complex (57). In this study, we have shown that disrupting the interaction between AHI-1 and BCR-ABL statistically significantly increased IM-induced apoptosis and reduced proliferation in *BCR-ABL*–transduced cells, indicating a positive regulatory role for the WD40 repeats in modulating IM response in CML. Of particular note is our previous observation that the highest levels and activity of endogenous BCR-ABL and AHI-1 occur in CML LSCs, with progressive downregulation as the cells differentiate (22,34,36). This finding suggests that it is crucial to the AHI-1–BCR-ABL cooperative activities in CML LSCs to generate a rapidly expanding clone of deregulated LSCs that are intrinsically more resistant to TKI treatment than their more-mature cells, potentially contributing to disease progression and drug resistance (Figure 7C).

Our finding that deletion of the N-terminus of AHI-1 prevents it from interacting with JAK2 in *BCR-ABL*$^+$ cells and sensitizes the cells to the apoptosis-inducing activity of IM implicates the AHI-1–JAK2 interaction in the innate IM-resistant phenotype of primitive human CML cells. However, we also showed that disruption of the ability of AHI-1 to interact with BCR-ABL has an even more pronounced effect on IM sensitivity than disruption of AHI-1's ability to interact with JAK2. This may be because of the reported ability of JAK2 to interact directly with BCR-ABL via its C-terminus in certain cell lines and thereby independently promote the transforming activity of BCR-ABL (7). The BCR-ABL–JAK2

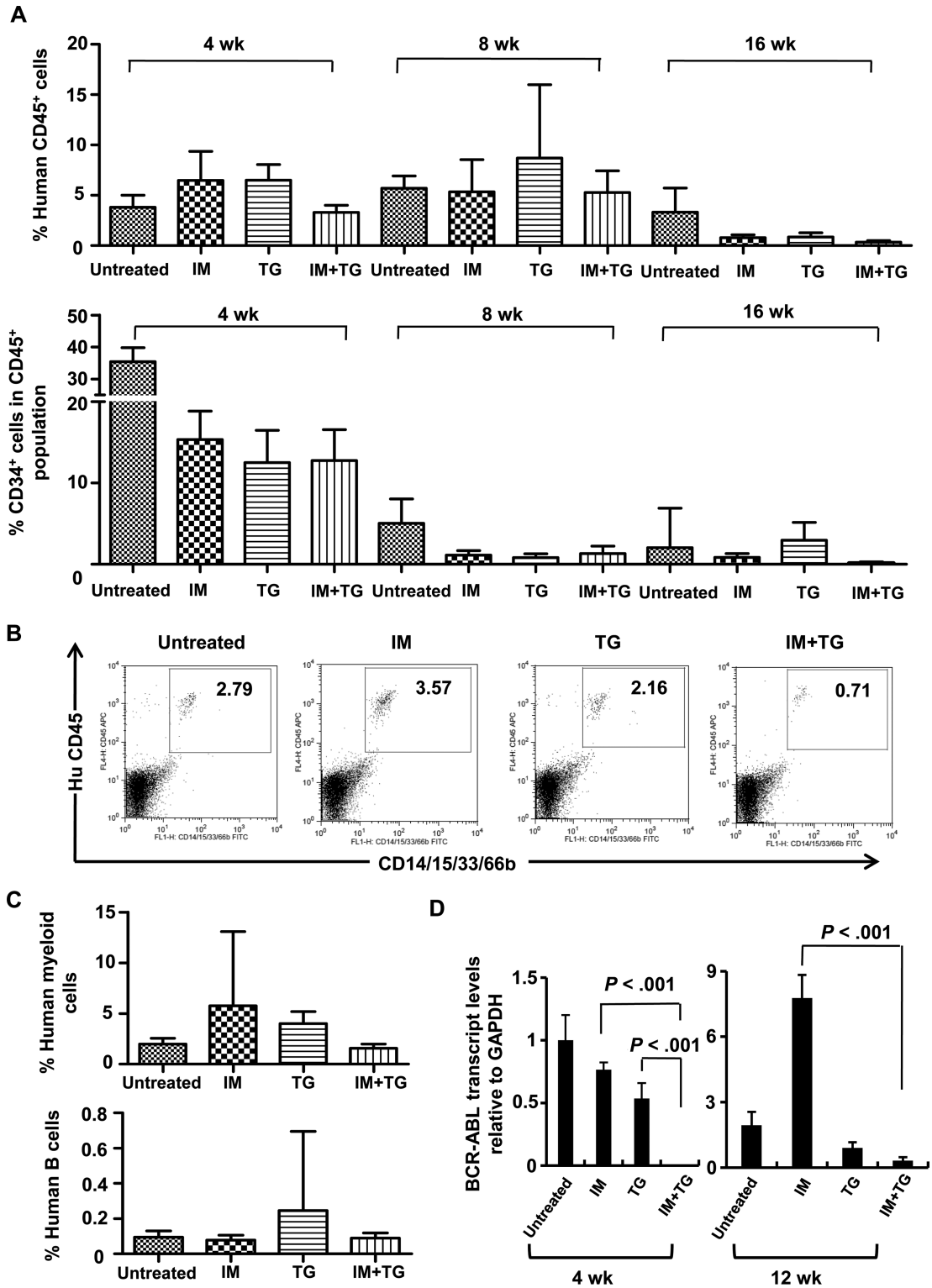

Figure 8. Elimination of chronic myeloid leukemia (CML) leukemic stem cells capable of long-term production of *BCR-ABL*$^+$ cells in immunodeficient mice using combined exposure to TG101209 (TG) and imatinib (IM). **A)** CD34$^+$ cells from three CML patients were cultured with 1.0 μM IM, 0.1 μM TG, IM plus TG, or without treatment for 3 days. Cells recovered were injected intravenously into NOD/SCID–interleukin 2 receptor γ–chain-deficient (NSG) mice (n = 3 mice per condition per patient sample). After 4, 8, 12, and 16 weeks, bone marrow (BM) aspirates were obtained, and the presence of human CD45$^+$ and CD34$^+$ cells was measured. **B)** Fluorescence-activated cell sorting profiles of regenerated human myeloid cells (CD45/CD14/15/33/66b$^+$) in the BM of representative mice analyzed 12 weeks posttransplant. **C)** The percentage of human myeloid (CD45/CD14/15/33/66b$^+$) and lymphoid cells (CD45/CD19/20$^+$) in the BM of representative mice analyzed 4 weeks posttransplant. **D)** *BCR-ABL* transcript levels measured by quantitative reverse transcription polymerase chain reaction in fluorescence-activated cell sorting–purified human CD45$^+$ cells obtained at 4 and 12 weeks posttransplant from the BM of mice injected with cells treated with inhibitors and those without. Data are means, and error bars represent 95% confidence intervals of six to nine measurements per condition. *P* values were calculated using a two-sided Student *t* test.

complex may thus be able to compensate, to some extent, for the sensitizing effect that disrupting the AHI-1–JAK2 interaction has on IM-induced apoptosis of *BCR-ABL*$^+$ cells. Interestingly, a recent study suggests that the BCR-ABL–mediated signaling pathways in CML cells are controlled by JAK2 through direct phosphorylation of tyrosine 177 of the BCR-ABL oncoprotein (9). It is unlikely that AHI-1 directly interacts with tyrosine 177 of BCR-ABL to mediate drug response of CML cells because AHI-1 doesn't contain a SH2 domain, which is required for interaction with tyrosine 177 of BCR-ABL, but rather interacts with BCR-ABL through the WD40 domain of AHI-1, as demonstrated in this study. However, it still remains to be determined if AHI-1 may regulate BCR-ABL activity through Y177 indirectly or through JAK2. Nevertheless, the observation of markedly increased apoptosis and reduced proliferation of *BCR-ABL*$^+$ cells exposed to TKIs by interrupting both AHI-1–JAK2 and AHI-1–BCR-ABL interactions indicates that AHI-1–mediated protein–protein interactions are required to mediate response/resistance of CML cells to TKIs (Figure 7C).

Thus, targeting JAK2 activity could be an ideal strategy to complement the inhibition of TK activity of BCR-ABL in primary CML stem and progenitor cells because the insensitivity of these cells to single TKI treatment is a potential source of disease persistence and relapse (Figure 7C) (8,14,15,26,27,58). Interestingly, BCR-ABL has been found to interact with the IL-3/GM-CSF receptor, which then contributes to the downstream activation of JAK2 (59). In addition, in primitive CML cells, BCR-ABL expression stimulates the production of IL-3, G-CSF, and GM-CSF, which, following binding to their cognate receptors, further contribute to CML progenitor cell resistance to TKIs by activation of the JAK2/STAT5 pathway (60,61). Recently, high STAT5 levels were also found to mediate acquired IM resistance in CML cells, and the STAT5 inhibitor, pimozide, was shown to reduce their survival (62,63).

Consistent with this prediction, we found that treatment of *AHI-1*–overexpressing K562 cells and IM-resistant K562 cells (no detectable BCR-ABL–TK mutations, but with increased expression of BCR-ABL and AHI-1) with IM in combination with a JAK2 inhibitor (TG) was more effective at inhibiting the growth of these cells than the same dose of either drug on its own. This enhanced inhibition of growth was mirrored by a correspondingly enhanced reduction in BCR-ABL, CRKL, JAK2, and STAT5 phosphorylation in the same cells treated with IM plus TG, as compared with those treated with IM or TG alone (Figure 2 and 3). Reduced protein expression of AHI-1 and JAK2 was also observed as a result of treatment with TG alone or the combination. Importantly, the AHI-1–BCR-ABL–JAK2 protein interaction complex was markedly interrupted in CML cells with IM plus TG, as compared with cells treated with IM or TG alone (Figure 2F). Together, these results indicate that dissociation of BCR-ABL and JAK2 kinases from AHI-1 can sensitize *BCR-ABL*$^+$ cells to IM. Additional experiments, using primary CML cells and both short- and long-term readouts in vitro and in vivo, confirmed that, in every case, the same drugs together were more effective in targeting early CML stem/progenitor cells than a TKI or JAK2 inhibitor alone. Combination treatment with TKIs to target BCR-ABL TK activity alone (IM plus DA or NL) was not able to achieve the statistically significant effects seen in CML stem/progenitor cells in response to targeting both BCR-ABL and JAK2 (Figure 6A). In particular, the TKI and TG combination resulted in statistically significant depletion of P-CRKL and P-STAT5 activity in CML stem/progenitor cells, as compared with TKIs alone (Figure 6C), providing further molecular evidence that suppressing both BCR-ABL and JAK2 activities in CML stem/progenitor cells is critical for eradication of these cells.

We also asked whether the combination of TG plus TKI treatment might be a better treatment strategy for CP patients who may be unlikely to respond to single TKIs because TKIs would fail to significantly reduce the LSC population. Such patients might thus benefit from a treatment that could effectively reduce the CML LSC burden, thereby escaping the development of TKI-resistant CML LSC. Our analysis of treatment-naive CD34$^+$ cells isolated from CML samples obtained at diagnosis from patients who subsequently proved to be clinically unresponsive to IM therapy provides direct support for this hypothesis. Even in cells from such patients, we found that TKI and TG in combination were capable of markedly reducing the numbers of TKI-resistant colonies in vitro and depleting their more-primitive precursors, including LTC-ICs and CML LSCs, capable of regenerating sustained populations of *BCR-ABL*$^+$ cells in NSG mice. Our study thus suggests an attractive strategy of TKI and TG in combination for treating CP CML patients who may develop IM resistance later. On the other hand, this combination may be less suitable for treating certain types of TKI-resistant patients whose resistance is due to the presence of a mutant kinase that is not responsive to known TKIs; in this case, a strategy that successfully targeted JAK2 may not be sufficient to be therapeutically effective. However, it has recently been reported that ponatinib, a third-generation of TKI, and DCC-2036, a "switch-control" inhibitor that potently inhibits both unphosphorylated and phosphorylated ABL by inducing a type 2 inactive conformation, retain efficacy against the majority of clinically relevant TKI-resistant mutants, including T315I (64,65). Their efficacy at targeting CML stem/progenitor cells remains to be determined. Because increased JAK2 activity and expression were observed in IM-resistant CML cells, a combination of DCC-2036 (or ponatinib) and TG may thus be an ideal approach to eliminate these critical resistant stem/progenitor cells. Interestingly, in vivo administration of TG and IM by 2-week oral treatment was highly effective in eliminating BV173 CML cells that can generate an aggressive leukemia in mice. A statistically significant prolonged survival of treated mice was obtained by the combination, whereas IM or TG alone was ineffective at preventing disease development (Figure 7B). These results suggest that the combination treatment may be more effective at targeting more-aggressive leukemic cells present in late stages of CML because it has been challenging to treat these late-stage patients by IM monotherapy (8,14,15,66).

The JAK2 inhibitor (TG) was originally designed to target JAK2 mutations in myeloproliferative disorders and has been reported to be highly effective against the JAK2 V617F mutation in polycythemia vera progenitors (67–69). In this study, we found that TG by itself had limited effects on inhibition of primary CD34$^+$ CML cells when the concentration of TG was nontoxic to primitive normal BM cells. This difference could be due to the BCR-ABL–mediated activation of other pathways in primitive CML cells, potentially including downstream effects on STAT5 in a JAK2 activation-independent manner (62,70). The additional

finding that AHI-1 strongly associates with JAK2 in the absence of BCR-ABL suggests that an AHI-1–JAK2 interaction may also play a role in regulating primitive normal hematopoietic cell signaling. This possibility is further reinforced by the finding that expression of *AHI-1* is normally downregulated during the initial phase of hematopoietic cell differentiation (36).

Some potential limitations of this study should be considered. First, the in vitro and in vivo studies of CML stem/progenitor cell response to TKIs and a JAK2 inhibitor presented here were confined to a relatively small number of CP CML patients' samples. These data are not robust, and the results must therefore be interpreted with due caution. In addition, leukemic stem and progenitor cell numbers vary from patient to patient, and this may directly affect response/resistance of these cells to single and combination treatments. A second limitation of this study is that the therapeutic window for the JAK2 inhibitor TG102109 is relatively small and there is a need for the development of more selective and less toxic JAK2 inhibitors. Nevertheless, it is of considerable interest that the combined effect of TKI and TG on primitive CML stem/progenitor cells is consistently superior (inhibitory) to their exposure to either agent alone. Taken together, the results strongly support a therapeutic role for TG plus a TKI, leading to more complete disease eradication for CML patients, particularly for those who are likely to develop TKI-resistant subclones if treated with a TKI alone.

References

1. Sawyers CL. Chronic myeloid leukemia. *N Engl J Med.* 1999;340(17):1330–1340.
2. Goldman JM, Melo JV. Chronic myeloid leukemia—advances in biology and new approaches to treatment. *N Engl J Med.* 2003;349(15):1451–1464.
3. Sloma I, Jiang X, Eaves AC, Eaves CJ. Insights into the stem cells of chronic myeloid leukemia. *Leukemia.* 2010;24(11):1823–1833.
4. Chen Y, Peng C, Sullivan C, Li D, Li S. Critical molecular pathways in cancer stem cells of chronic myeloid leukemia. *Leukemia.* 2010;24(9):1545–1554.
5. Sattler M, Griffin JD. Molecular mechanisms of transformation by the BCR-ABL oncogene. *Semin Hematol.* 2003;40(2 Suppl 2):4–10.
6. Van Etten RA. Oncogenic signaling: new insights and controversies from chronic myeloid leukemia. *J Exp Med.* 2007;204(3):461–465.
7. Samanta AK, Lin H, Sun T, Kantarjian H, Arlinghaus RB. Janus kinase 2: a critical target in chronic myelogenous leukemia. *Cancer Res.* 2006;66(13):6468–6472.
8. Woolfson A, Jiang X. Targeting the chronic myeloid leukemia stem cells: a paradigm for the curative treatment of human malignancies. In: Koschmeider S, Krug U, eds. *Myeloid Leukemia—Basic Mechanisms of Leukemogenesis*. New York: INTECH Open Access Publisher; 2011:85–110.
9. Samanta A, Perazzona B, Chakraborty S, et al. Janus kinase 2 regulates Bcr-Abl signaling in chronic myeloid leukemia. *Leukemia.* 2011;25(3):463–472.
10. Druker BJ, Tamura S, Buchdunger E, et al. Effects of a selective inhibitor of the Abl tyrosine kinase on the growth of Bcr-Abl positive cells. *Nat Med.* 1996;2(5):561–566.
11. Druker BJ, Guilhot F, O'Brien SG, et al. Five-year follow-up of patients receiving imatinib for chronic myeloid leukemia. *N Engl J Med.* 2006;355(213):2408–2417.
12. Shah NP, Tran C, Lee FY, Chen P, Norris D, Sawyers CL. Overriding imatinib resistance with a novel ABL kinase inhibitor. *Science.* 2004;305(5682):399–401.
13. Weisberg E, Manley PW, Breitenstein W, et al. Characterization of AMN107, a selective inhibitor of native and mutant Bcr-Abl. *Cancer Cell.* 2005;7(2):129–141.
14. Gorre ME, Mohammed M, Ellwood K, et al. Clinical resistance to STI-571 cancer therapy caused by BCR-ABL gene mutation or amplification. *Science.* 2001;293(5531):876–880.
15. Deininger M, Buchdunger E, Druker BJ. The development of imatinib as a therapeutic agent for chronic myeloid leukemia. *Blood.* 2005;105(7):2640–2653.
16. Jiang X, Saw KM, Eaves A, Eaves C. Instability of BCR-ABL gene in primary and cultured chronic myeloid leukemia stem cells. *J Natl Cancer Inst.* 2007;99(9):680–693.
17. Hughes TP, Kaeda J, Branford S, et al. Frequency of major molecular responses to imatinib or interferon alfa plus cytarabine in newly diagnosed chronic myeloid leukemia. *N Engl J Med.* 2003;349(15):1423–1432.
18. Rousselot P, Huguet F, Rea D, et al. Imatinib mesylate discontinuation in patients with chronic myelogenous leukemia in complete molecular remission for more than 2 years. *Blood.* 2007;109(1):58–60.
19. Mahon FX, Rea D, Guilhot J, et al. Discontinuation of imatinib in patients with chronic myeloid leukaemia who have maintained complete molecular remission for at least 2 years: the prospective, multicentre Stop Imatinib (STIM) trial. *Lancet Oncol.* 2010;11(11):1029–35.
20. Tang M, Foo J, Gonen M, Guilhot J, Mahon FX, Michor F. Selection pressure exerted by imatinib therapy leads to disparate outcomes of imatinib discontinuation trials. *Haematologica.* 2012;97(10):1553–1561.
21. Graham SM, Jorgensen HG, Allan E, et al. Primitive, quiescent, Philadelphia-positive stem cells from patients with chronic myeloid leukemia are insensitive to STI571 in vitro. *Blood.* 2002;99(1):319–325.
22. Copland M, Hamilton A, Elrick LJ, et al. Dasatinib (BMS-354825) targets an earlier progenitor population than imatinib in primary CML, but does not eliminate the quiescent fraction. *Blood.* 2006;107(11):4532–4539.
23. Jorgensen HG, Allan EK, Jordanides NE, Mountford JC, Holyoake TL. Nilotinib exerts equipotent antiproliferative effects to imatinib and does not induce apoptosis in CD34+ CML cells. *Blood.* 2007;109(9):4016–4019.
24. Bhatia R, Holtz M, Niu N, et al. Persistence of malignant hematopoietic progenitors in chronic myelogenous leukemia patients in complete cytogenetic remission following imatinib mesylate treatment. *Blood.* 2003;101(12):4701–4707.
25. Chu S, Xu H, Shah NP, et al. Detection of BCR-ABL kinase mutations in CD34+ cells from chronic myelogenous leukemia patients in complete cytogenetic remission on imatinib mesylate treatment. *Blood.* 2005;105(5):2093–2098.
26. Chu S, McDonald T, Lin A, et al. Persistence of leukemia stem cells in chronic myelogenous leukemia patients in prolonged remission with imatinib treatment. *Blood.* 2011;118(20):5565–5572.
27. Chomel JC, Bonnet ML, Sorel N, et al. Leukemic stem cell persistency in chronic myeloid leukemia patients with sustained undetectable molecular residual disease. *Blood.* 2011;119(13):2964–2965.
28. Zhang B, Strauss AC, Chu S, et al. Effective targeting of quiescent chronic myelogenous leukemia stem cells by histone deacetylase inhibitors in combination with imatinib mesylate. *Cancer Cell.* 2010;17(5):427–442.
29. Li L, Wang L, Li L, et al. Activation of p53 by SIRT1 inhibition enhances elimination of CML leukemia stem cells in combination with Imatinib. *Cancer Cell.* 2012;21(2):266–281.
30. Chen Y, Hu Y, Zhang H, Peng C, Li S. Loss of the Alox5 gene impairs leukemia stem cells and prevents chronic myeloid leukemia. *Nat Genet.* 2009;41(7):783–792.
31. Duy C, Hurtz C, Shojaee S, et al. BCL6 enables Ph+ acute lymphoblastic leukaemia cells to survive BCR-ABL1 kinase inhibition. *Nature.* 2011;473(7347):384–388.
32. Corbin AS, Agarwal A, Loriaux M, Cortes J, Deininger MW, Druker BJ. Human chronic myeloid leukemia stem cells are insensitive to imatinib despite inhibition of BCR-ABL activity. *J Clin Invest.* 2011;121(3):396–409.
33. Hamilton A, Helgason GV, Schemionek M, et al. Chronic myeloid leukemia stem cells are not dependent on Bcr-Abl kinase activity for their survival. *Blood.* 2012;119(6):1501–1510.
34. Jiang X, Zhao Y, Smith C, et al. Chronic myeloid leukemia stem cells possess multiple unique features of resistance to BCR-ABL targeted therapies. *Leukemia.* 2007;21(5):926–935.
35. Jiang X, Smith C, Eaves A, Eaves C. The challenges of targeting chronic myeloid leukemia stem cells. *Clin Lymphoma Myeloma.* 2007;7(Suppl 2):S71–S80.
36. Jiang X, Zhao Y, Chan WY, et al. Deregulated expression in Ph^+ human leukemias of AHI-1, a gene activated by insertional mutagenesis in mouse models of leukemia. *Blood.* 2004;103(10):3897–3904.

37. Esmailzadeh S, Jiang X. AHI-1: a novel signaling protein and potential therapeutic target in human leukemia and brain disorders. *Oncotarget*. 2011;12(12):918–934.
38. Jiang X, Hanna Z, Kaouass M, Girard L, Jolicoeur P. Ahi-1, a novel gene encoding a modular protein with WD40-repeat and SH3 domains, is targeted by the Ahi-1 and Mis-2 provirus integrations. *J Virol.* 2002;76(18):9046–9059.
39. Zhou LL, Zhao Y, Ringrose A, et al. AHI-1 interacts with BCR-ABL and modulates BCR-ABL transforming activity and imatinib response of CML stem/progenitor cells. *J Exp Med.* 2008;205(11):2657–2671.
40. Dugray A, Geay JF, Foudi A, et al. Rapid generation of a tetracycline-inducible BCR-ABL defective retrovirus using a single autoregulatory retroviral cassette. *Leukemia.* 2001;15(10):1658–1662.
41. Petzer AL, Eaves CJ, Lansdorp PM, Ponchio L, Barnett MJ, Eaves AC. Characterization of primitive subpopulations of normal and leukemic cells present in the blood of patients with newly diagnosed as well as established chronic myeloid leukemia. *Blood.* 1996;88(6):2162–2171.
42. Hamilton A, Elrick L, Myssina S, et al. BCR-ABL activity and its response to drugs can be determined in CD34+ CML stem cells by CrkL phosphorylation status using flow cytometry. *Leukemia.* 2006;20(6):1035–1039.
43. Pardanani A, Hood J, Lasho T, et al. TG101209, a small molecule JAK2-selective kinase inhibitor potently inhibits myeloproliferative disorder-associated JAK2V617F and MPLW515L/K mutations. *Leukemia.* 2007;21(8):1658–1668.
44. Wu J, Meng F, Lu H, et al. Lyn regulates BCR-ABL and Gab2 tyrosine phosphorylation and c-Cbl protein stability in imatinib-resistant chronic myelogenous leukemia cells. *Blood.* 2008;111(7):3821–3829.
45. Donato NJ, Wu JY, Stapley J, et al. BCR-ABL independence and LYN kinase overexpression in chronic myelogenous leukemia cells selected for resistance to STI571. *Blood.* 2003;101(2):690–698.
46. Wu J, Meng F, Kong LY, et al. Association between imatinib-resistant BCR-ABL mutation-negative leukemia and persistent activation of LYN kinase. *J Natl Cancer Inst.* 2008;100(13):926–939.
47. Fenouille N, Puissant A, Dufies M, et al. Persistent activation of the Fyn/ERK kinase signaling axis mediates imatinib resistance in chronic myelogenous leukemia cells through upregulation of intracellular SPARC. *Cancer Res.* 2010;70(23):9659–9670.
48. Holyoake T, Jiang X, Eaves C, Eaves A. Isolation of a highly quiescent subpopulation of primitive leukemic cells in chronic myeloid leukemia. *Blood.* 1999;94(6):2056–2064.
49. Jiang X, Forrest D, Nicolini F, et al. Properties of $CD34^+$ CML stem/progenitor cells that correlate with different clinical responses to imatinib mesylate. *Blood.* 2010;116(12):2112–2121.
50. Dazzi F, Capelli D, Hasserjian R, et al. The kinetics and extent of engraftment of chronic myelogenous leukemia cells in non-obese diabetic/severe combined immunodeficiency mice reflect the phase of the donor's disease: an in vivo model of chronic myelogenous leukemia biology. *Blood.* 1998;92(4):1390–1396.
51. Shultz LD, Lyons BL, Burzenski LM, et al. Human lymphoid and myeloid cell development in NOD/LtSz-*scid IL2Rγ* ^{null} mice engrafted with mobilized human hemopoietic stem cells. *J Immunol.* 2005;174(10):6477–6489.
52. Vomastek T, Schaeffer HJ, Tarcsafalvi A, Smolkin ME, Bissonette EA, Weber MJ. Modular construction of a signaling scaffold: MORG1 interacts with components of the ERK cascade and links ERK signaling to specific agonists. *Proc Natl Acad Sci U S A.* 2004;101(18):6981–6986.
53. Ritterhoff S, Farah CM, Grabitzki J, Lochnit G, Skurat AV, Schmitz ML. The WD40-repeat protein Han11 functions as a scaffold protein to control HIPK2 and MEKK1 kinase functions. *EMBO J.* 2010;29(22):3750–3761.
54. Huang CC, Liu CH, Chuang NN. An enhanced association of RACK1 with Abl in cells transfected with oncogenic ras. *Int J Biochem Cell Biol.* 2008;40(3):423–431.
55. Ferland RJ, Eyaid W, Collura RV, et al. Corrigendum: Abnormal cerebellar development and axonal decussation due to mutations in AHI1 in Joubert syndrome. *Nat Genet.* 2004;36(9):1008–1013.
56. Valente EM, Brancati F, Silhavy JL, et al. AHI1 gene mutations cause specific forms of Joubert syndrome-related disorders. *Ann Neurol.* 2006;59(3):527–534.
57. Sheng G, Xu X, Lin Y-F, et al. Huntingtin-associated protein 1 interacts with Ahi1 to regulate cerebellar and brainstem development in mice. *J Clin Invest.* 2008;118(8):2785–2795.
58. O'Hare T, Zabriskie MS, Eiring AM, Deininger WD. Pushing the limits of targeted therapy in chronic myeloid leukaemia. *Nat Rev Cancer*. 2012;24:12(8):513–526.
59. Wilson-Rawls J, Liu J, Laneuville P, Arlinghaus RB. P210 Bcr-Abl interacts with the interleukin-3 beta c subunit and constitutively activates Jak2. *Leukemia.* 1997;11(Suppl 3):428–431.
60. Jiang X, Lopez A, Holyoake T, Eaves A, Eaves C. Autocrine production and action of IL-3 and granulocyte colony-stimulating factor in chronic myeloid leukemia. *Proc Natl Acad Sci U S A.* 1999;96(22):12804–12809.
61. Wang Y, Cai D, Brendel C, et al. Adaptive secretion of granulocyte-macrophage colony-stimulating factor (GM-CSF) mediates imatinib and nilotinib resistance in BCR/ABL^+ progenitors via JAK-2/STAT-5 pathway activation. *Blood.* 2007;109(5):2147–2155.
62. Warsch W, Kollmann K, Eckelhart E, et al. High STAT5 levels mediate imatinib resistance and indicate disease progression in chronic myeloid leukemia. *Blood.* 2011;117(12):3409–3420.
63. Nelson EA, Walker SR, Weisberg E, et al. The STAT5 inhibitor pimozide decreases survival of chronic myelogenous leukemia cells resistant to kinase inhibitors. *Blood.* 2011;117(12):3421–3429.
64. O'Hare T, Shakespeare WC, Zhu X, et al. AP24534, a pan-BCR-ABL inhibitor for chronic myeloid leukemia, potently inhibits the T315I mutant and overcomes mutation-based resistance. *Cancer Cell.* 2009;6(5):401–412.
65. Chan WW, Wise SC, Kaufman MD, et al. Conformational control inhibition of the BCR-ABL1 tyrosine kinase, including the gatekeeper T315I mutant, by the switch-control inhibitor DCC-2036. *Cancer Cell.* 2011;12(4):556–568.
66. Forrest DL, Jiang X, Eaves CJ, Smith CL. An approach to the management of chronic myeloid leukemia in British Columbia. *Curr Oncol.* 2008;15(2):48–55.
67. Geron I, Abrahamsson AE, Barroga CF, et al. Selective inhibition of JAK2-driven erythroid differentiation of polycythemia vera progenitors. *Cancer Cell.* 2008;13(4):321–330.
68. Wernig G, Kharas MG, Okabe R, et al. Efficacy of TG101348, a selective JAK2 inhibitor, in treatment of a murine model of JAK2V617F-induced polycythemia vera. *Cancer Cell.* 2008;13(4):311–320.
69. Tefferi A. JAK inhibitors for myeloproliferative neoplasms: clarifying facts from myths. *Blood.* 2012;119(12):2721–2730.
70. Sillaber C, Gesbert F, Frank DA, Sattler M, Griffin JD. STAT5 activation contributes to growth and viablility in Bcr/Abl-transformed cells. *Blood.* 2000;95(6):2118–2125.

Funding

This work was funded by the Canadian Cancer Society (grant 700289), in part by the Canadian Institutes of Health Research, the Leukemia & Lymphoma Society of Canada, and the Cancer Research Society (XJ), the Canadian Cancer Society Research Institute (AE, XJ, CE), Cancer Research UK Programme grant C11074/A11008 (TLH), the Glasgow Experimental Cancer Medicine Centre, which is funded by Cancer Research UK and by the Chief Scientist's Office (Scotland), and Cancer Research UK grant C973/A9894 (JP, JS). M. Chen was supported by a fellowship from Lymphoma Foundation Canada, and P. Gallipoli was supported by Medical Research Council grant G1000288. X. Jiang was a Michael Smith Foundation for Health Research Scholar.

Notes

M. Chen and P. Gallipoli contributed equally to this work.

The authors have no conflicting financial interests.

The authors thank the Stem Cell Assay Laboratory for cell processing and cryopreservation of samples; all members of the Leukemia/BMT Program of British Columbia, the Hematology Cell Bank of British Columbia Vancouver, BC, Canada and UK haematologists for providing patient samples; the Terry Fox Laboratory and Paul O'Gorman LRC FACS Facilities for assistance in cell sorting; Novartis for providing IM, NL, and IL-3; British-Myers Squibb for DA, TargeGen Inc for TG, STEMCELL Technologies for culture reagents; and Dr Y. Xing, Y. Zhang, and C. Bray for valuable discussion.

Affiliations of authors: Terry Fox Laboratory (MChen, DD, IS, MChan, DL, AR, HMW, KL, HN, KMS, AE, CJE, XJ) and Leukemia/BMT Program of British Columbia, Division of Hematology (DLF, MJB), British Columbia Cancer Agency, Vancouver, BC, Canada; Paul O'Gorman Leukemia Research Centre, College of Medical, Veterinary and Life Sciences (PG, HJ, TLH) and Cancer Research UK Clinical Trials Unit (JP, JS), University of Glasgow, Glasgow, UK; Department of Medicine (DLF, MJB, AE, CJE, XJ) and Department of Medical Genetics (CJE, XJ), University of British Columbia, Vancouver, BC, Canada; Department of Hematology and Biological Oncology, University of Poitiers, INSERM U935, Poitiers, France (AT); Department of Molecular Pathology, University of Texas MD Anderson Cancer Center, Houston, TX (RA).